DOKUZ EYLÜL UNIVERSITY
GRADUATE SCHOOL OF NATURAL AND APPLIED SCIENCES

SEGMENTATION IN ABDOMINAL MEDICAL IMAGES

by
Aykut KOCAOĞLU

July, 2007
İZMİR

SEGMENTATION IN ABDOMINAL MEDICAL IMAGES

A Thesis Submitted to the
Graduate School of Natural and Applied Sciences of Dokuz Eylül University
In Partial Fulfillment of the Requirements for the Degree of Master of Science
in Electrical and Electronics Engineering

by

Aykut KOCAOĞLU

July, 2007

İZMİR

M.Sc THESIS EXAMINATION RESULT FORM

We have read the thesis entitled **"SEGMENTATION IN ABDOMINAL MEDICAL IMAGES"** completed by **AYKUT KOCAOĞLU** under supervision of **ASSIST. PROF. DR. GÜLESER KALAYCI DEMİR** and we certify that in our opinion it is fully adequate, in scope and in quality, as a thesis for the degree of Master of Science.

.....

Assist. Prof. Dr. Güleser Kalaycı Demir

....

(Jury Member) (Jury Member)

Prof. Dr. Cahit HELVACI
Director
Graduate School of Natural and Applied Sciences

ACKNOWLEDGEMENTS

This thesis would not have been possible without the kind support, the trenchant critiques, the probing questions, and the remarkable patience of may thesis advisor - Assist. Prof. Dr. Güleser Kalaycı Demir.

I also would like to thank Prof. Dr. Cüneyt Güzeliş, Prof. Dr. Oğuz Dicle and Dr. Hatice Doğan for their valuable guidance during preparation of this thesis. Their intellectual contribution to my development has been invaluable.

Furthermore, special thanks go to Rsrch. Assist. Alper Selver for his continuous friendship and generous support during my two year education at Dokuz Eylül University.

I would also like to express my deep gratitude also to my esteemed colleagues and friends Mehmet Ölmez, Ömer Karal and Halil Yeltekin. They have all been a model of patience and understanding.

Last but not least, I offer my sincere thanks to my loving family. Throughout all my endeavors, their love, support, guidance, and endless patience have been truly inspirational. This thesis is simply impossible without them.

Aykut KOCAOĞLU

SEGMENTATION IN ABDOMINAL MEDICAL IMAGES

ABSTRACT

Abdominal medical image segmentation is the process of labeling each voxel in a medical image dataset to indicate its tissue type or anatomical structure. Identifying organs from abdominal Computed Tomography (CT) datasets is one of the essential steps for surgical planning. However, due to gray level similarity of adjacent organs, injection of contrast material and partial volume effects; robust segmentation of abdominal organs is a very difficult task. In this thesis, segmentation of liver parenchyma, which is essential for live donor liver transplantation surgery, is studied. Three different automatic and semi-automatic hybrid liver segmentation algorithms are proposed and their performances are compared. All proposed algorithms have three stages; namely, preprocessing, classification/thresholding and post-processing. In the first algorithm, k-means clustering is used as a classifier. In the second algorithm, Multi Layer Perceptron, which is a more complex classifier, is used. In the third algorithm dynamical thresholding is used to identify liver parenchyma.

The first algorithm is able to deal with contrast variations. In addition, it is worth to say that this algorithm is much faster supporting applicability for clinical usage. The second and third algorithms are able to deal with not only contrast variations but also atypical liver shapes. These capabilities are provided by the patient oriented structure which learns the characteristics of a patient dataset for each slice in parallel to the segmentation process and adapts its parameters according to these characteristics.

Keywords : Liver Segmentation, Computed Tomography, Multi Layer Perceptron Network, k-means, Dynamical Thresholding

KARIN BÖLGESİNE AİT TIBBİ GÖRÜNTÜLERDE BÖLÜTLEME

ÖZ

Karın bölgesine ait tıbbi görüntülerin bölütlenmesi her görüntü veri setindeki voksellerin hangi dokuya ait olduğunun etiketlenmesi ve anatomik yapılarının gösterilmesi işlemidir. Ameliyat öncesi planlamada organların bilgisayarlı tomografi görüntülerinden tanımlanması önemlidir. Ancak; bitişik organların gri seviye benzerlikleri, hastaya opak madde enjekte edilmesi ve parçalı hacim etkisi gibi sebeplerle organların doğru bir şekilde bölütlenmesi zor bir işlemdir. Bu tezde, karaciğer nakli ameliyatlarından önce gerekli olan karaciğer dokusunun tanımlanması ele alınmış, otomatik ve yarı otomatik olmak üzere üç ayrı algoritma önerilmiş ve başarımları karşılaştırılmıştır. Her üç algoritma da ön-işleme, sınıflama/eşikleme ve son-işleme olmak üzere üç aşamadan oluşmaktadır. İlk algoritmada, sınıflayıcı olarak k-ortalamalar yöntemi kullanılırken; ikinci algoritmada, daha karmaşık bir sınıflayıcı olan çok katmanlı algılayıcı kullanılmıştır. Üçüncü algoritmada ise karaciğer dokusunu tanınması için dinamik eşikleme yöntemi kullanılmıştır.

Birinci algoritma karşıtlık değişimlerine karşı dayanıklıdır. Aynı zamanda, bu algoritma daha hızlı çalıştığı için klinik uygulanabilirlik açısından daha iyidir. İkinci ve üçüncü algoritmalar ise hem karşıtlık değişimlerine hem de tipik olmayan karaciğer şekillerine karşı dayanıklıdır. Bu özellikler hasta veri setinin karakteristiğinin bölütleme işlemine paralel öğrenilmesi ve parametrelerin bu karakteristiğe adapte olmasıyla sağlanmaktadır.

Anahtar kelimeler : Karaciğer Bölütleme, Bilgisayarlı Tomografi, Çok Katmanlı Algılayıcı, K-ortalamalar, Dinamik Eşikleme

CONTENTS

Page

THESIS EXAMINATION RESULT FORM ii
ACKNOWLEDGEMENTS iii
ABSTRACT iv
ÖZ v

CHAPTER ONE – INTRODUCTION 1

CHAPTER TWO – ANATOMY OF THE LIVER 7

2.1 Liver 7

2.2 Flow of Blood 8

2.3 Regeneration 8

2.4 Liver Surgery Planning and Donor Evaluation 8

2.5 Liver Surgery Procedure 9
2.5.1 Liver Segmentation 9
2.5.2 Vessel extraction and Couinaud's Classification 10
2.5.3 Volume Calculations 11
2.5.4 Visualization 11

CHAPTER THREE – OVERVIEW OF ABDOMINAL ORGAN SEGMENTATION AND ITS CHALLENGES 12

3.1 Identification Methods & Challenges 12
3.1.1 Manual Identification 12
3.1.2 Automatic Identification 12

3.2 Overview of Abdominal Organ Segmentation 14

CHAPTER FOUR– PROPOSED LIVER SEGMENTATION ALGORITHMS..... 16

4.1 K-means Clustering Based Segmentation of Liver 16
4.1.1 Patient Datasets 16
4.1.2 Segmentation of the Liver 17
4.1.2.1 Pre-processing..... 17
4.1.2.2 Classification of the Liver..... 19
4.1.2.3 Post-processing 20
4.1.3 Evaluation..... 21

4.2 Patient Oriented and Robust Semi-Automatic Liver Segmentation using Multi Layer Perceptron..... 23
4.2.1 Patient Datasets..... 23
4.2.2 Segmentation of the Liver 23
4.2.2.1 Pre-processing 24
4.2.2.1.1 Removing the Fat tissue 24
4.2.2.1.2 Removing the Spine and the Ribs 25
4.2.2.1.3 Removing the Right Kidney 26
4.2.2.1.3 ROI Selection 30
4.2.2.2 Classification of the Liver..... 30
4.2.2.2.1 Initial Image Segmentation 31
4.2.2.2.2 Segmentation with Multi Layer Perceptron (MLP) 32
4.2.2.3 Post-processing 36
4.2.3 Evaluation 38

4.3 Proposed Dynamical Thresholding based Liver Segmentation 40
4.3.1 Pre-processing..... 40
4.3.2 Dynamical Thresholding..... 41

4.3.3 Post-processing..... 41
4.3.4 Evaluation..... 43

4.4 Comparison of Three Algorithms..... 44

CHAPTER FIVE– CONCLUSION 45

REFERENCES..... 47

CHAPTER ONE
INTRODUCTION

In recent years; due to rapid evolution of computer science and image acquisition techniques, radiologists prefer dealing with digital images rather than analog films. Evolution of digital image processing and visualization techniques gives radiologists the advantage of using new techniques.

Anatomical structure of human body can be effectively determined by Computer Tomography (CT), Magnetic Resonance Imaging (MR) and Functional Magnetic Resonance Imaging (FMRI). Datasets such as in Figure 1.1 obtained from these kinds of equipments are used to form three-dimensional (3D) images via various visualization techniques. These datasets are used not only imaging but also diagnosis, surgical planning, computer guided surgery, planning of radiotherapy, etc.

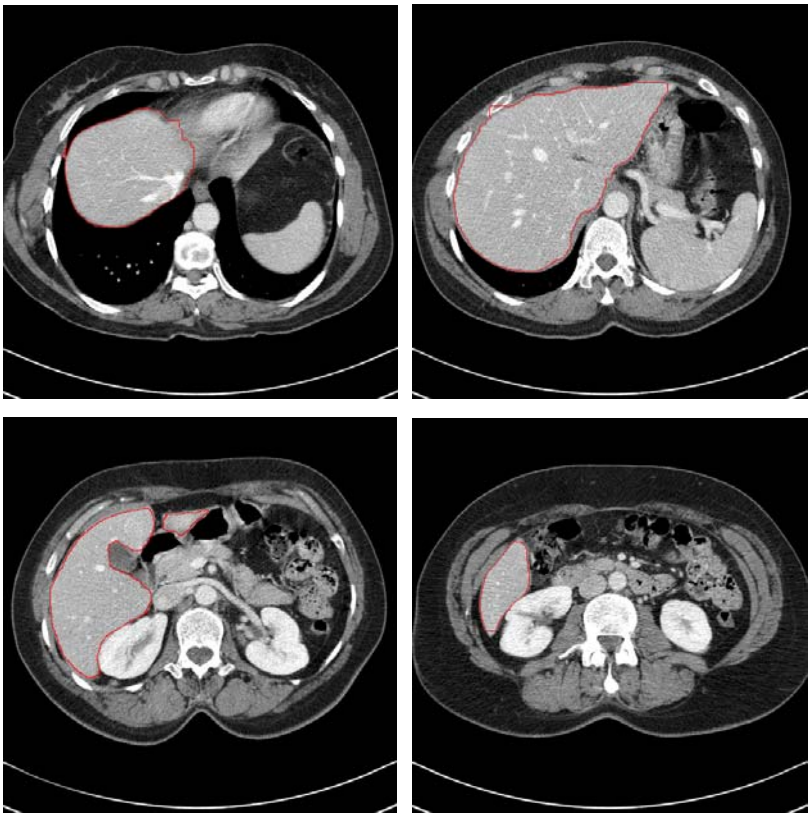


Figure 1.1 Sample abdominal CT images where liver is encircled with red

Segmentation is the process of labeling each voxel in a medical image dataset to indicate its tissue type or anatomical structure. However; due to the problems such as sampling, noise, low contrast, caused by medical equipments, it is difficult and\or sometimes impossible to identify anatomical structures.

In this thesis, identification of liver parenchyma, which is essential for live donor liver transplantation surgery, is focused.

Live donor liver transplantation is a procedure where a healthy voluntary donor gives a part of his or her liver to another person. Measurement of the liver volume and analysis of the liver vasculature are important stages to decide whether a candidate for transplantation is suitable or not. Generally, liver volume information is used to avoid size incompatibility between donor and patient, and vasculature analysis in Three Dimension (3D) is used for pre-evaluation of surgery.

Computed Tomography (CT) with contrast medium injection is currently the most widely used radiographic technique for the rendering of liver parenchyma, vessels and tumors in living liver transplantation donors. Before 3D rendering of the vasculature and the measurement of liver volume, accurate segmentation of the liver from surrounding tissues and organs is necessary. Since the number of image slices used for 3D rendering is very large, manual segmentation of the liver on each slice is time consuming and tedious. Also the results highly depend on the skill of the operator. Therefore, an automatic segmentation procedure to segment the liver in all slices is needed.

Besides its several advantages over manual segmentation, automatic segmentation of the liver is very challenging. These challenges arise from the following difficulties: First of all, the gray level values of adjacent organs of the liver are similar to each other (Figure 1.2 a-1.2 b). This similarity reduces the performance of thresholding techniques dramatically. Secondly, due to the injection of contrast media and/or different modality settings, the liver (and all other tissues) may have different gray-level values for different patient datasets, or even in different slices of

the same dataset (Figure 1.2 a-1.2 c). These effects prevent the usage of the gray level dependent segmentation techniques. Finally, the anatomical structure of the liver in different image slices is different and its shape can vary significantly from patient to patient (Fig. 1.2 a-1.2 b). Even two or three separate regions can be seen in the same slice (Fig. 1.2 c). Moreover, it is reported in (Soler et al., 2005) that around 15% of the patients have atypical liver shapes (i.e. unusual size or orientation of the liver, liver shape after segmentectomy) (Fig. 1.2 d). Thus, traditional shape based segmentation techniques are not enough to segment the liver efficiently.

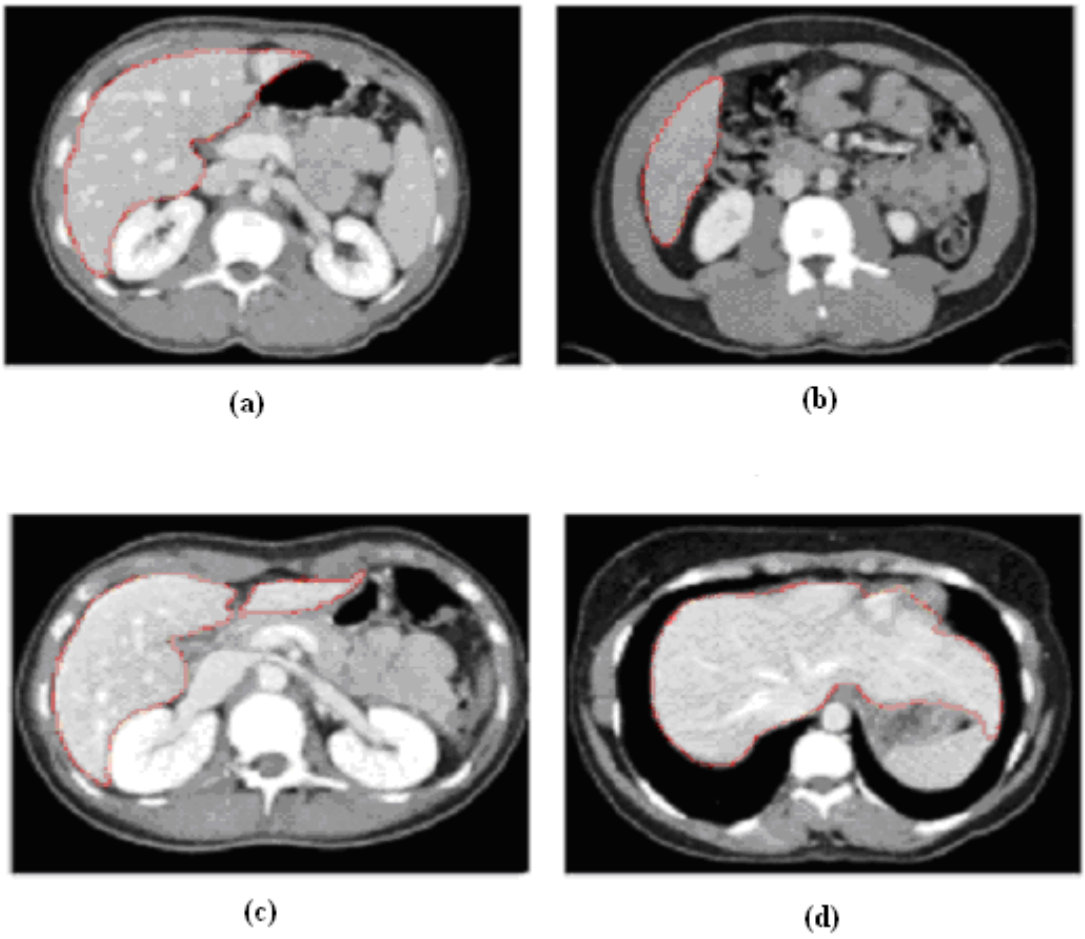


Figure 1.2 Examples of abdominal CT images (a) Very low contrast between liver and vena cava. (b) Low contrast between liver and muscle tissue (c) High contrast between liver and adjacent tissues (i.e. right kidney, muscle, vena cava) (d) Atypical liver shape that causes unclear boundary with spleen.

Our strategy for overcoming these difficulties involves segmentation methods which should not utilize a common parameter set found from all patient datasets. Instead, the method should be capable of adapting the parameter set to each patient.

The main reason for this approach is that the ranges of the parameter values differ significantly from patient to patient, and these wide ranges decrease the efficiency of the method when one utilizes a common parameter set for all patients.

Thus, three methods which examines and adapts its parameters according to each patient are proposed. This approach is called as patient-oriented segmentation. The first method learns dataset characteristics prior to the classification process. However, the second and third methods learn the dataset characteristics in parallel to segmentation process, and adapts its parameters to these characteristics in a slice-by-slice manner.

In the literature, different automatic and semi-automatic methods have been developed and performed for the segmentation of the liver from contrast enhanced CT series. These methods include but not limited to morphological techniques (Bae, Giger, Chen & Kahn, 1993 -Gao, Heath, Kuszyk & Fishman, 1996 - Lim, Jeong, Ho, 2005 - Masumoto et al., 2003), deformable models (Montagnat, Delingette, 1996 - Chou et al., 1995 - Soler et. al., 2005 - Gao, Kosaka & Kak, 2000) and neural networks (Tsai, 1994 – Husain & Shigeru, 2000- Lee, Chung & Tsai, 2003 - Koss, Newman, Johnson, & Kirch, 1999). However, neither in semi-automatic, nor in automatic algorithms, the problems of atypical liver shapes, different modality characteristics and datasets with low contrast adjacent tissues is handled together. Therefore, they do not deal with the all variations in contrast enhanced CT images at the same time.

Morphological techniques combined with gray level thresholding are used in (Bae et al., 1993) while in (Gao, Heath et al., 1996) and (Lim et al., 2005) these are combined with a parametrically deformable contour model which is used for boundary refinement. Although the method proposed in (Gao, Heath et al., 1996) is reported to be successful in most of the cases, a mean gray level value assumption is made for the liver at the intermediate levels of the algorithm. This assumption limits its use when the liver is more attenuating (brighter) due to the contrast media. Deformable contour models are also used by (Montagnat et al., 1996) and (Chou et

al., 1995). However the need for setting some seed points and parameters such as maximum gradient or time threshold makes it hard to use for radiologists. In (Soler et. al., 2005), an automatic algorithm is proposed using deformable models; however this method does not provide correct automatic result for atypical liver shapes. Artificial neural networks are used for gray level classification in (Tsai, 1994) and for feature based recognition in (Husain et al., 2000). The technique proposed in (Tsai, 1994) is semi-automatic and require more than one manually segmented image as training data prior to the automated process. The method in (Husain et. al., 2000) is not patient oriented and training is done with a limited set of images. Due to the high variation of image characteristics, a larger and more diverse database is recommended to generalize this system for reliable performance. A contextual neural network with a high segmentation performance is proposed in (Lee et al., 2003), but the results show that it fails where the gray level of the desired region is too close to the adjacent tissues. Recently, Seo et al. (Seo, Ludeman, Park & Park, 2004) proposed a fully automatic algorithm by determining the spine first and then by using it as a reference point for segmenting the liver using morphological operators, multimodal thresholding and a decision rule.

In this thesis, we propose three algorithms that can automatically/semi-automatically segment the liver in contrast enhanced CT series. The first algorithm is able to deal with contrast variations. The capability is provided by patient oriented structure which learns the characteristics of a patient dataset prior to the classification process. In addition, it is worth to say that this algorithm is much more faster supporting applicability for clinical usage. The second and third algorithms are able to deal with not only contrast variations but also atypical liver shapes. These capabilities are provided by the patient oriented structure which learns the characteristics of a patient dataset for each slice in parallel to the segmentation process and adapts its parameters according to these characteristics. First segmentation algorithm combines classification of pixels (using an unsupervised clustering method i.e. k-means) with adjacent slice information, (obtained by skeletonization) via morphological reconstruction. In the second algorithm, a more complex classifier (Multi Layer Perceptron Network - MLP) is developed for the

datasets where the K-means clustering gives insufficient results. Here, the neural network is designed to use features extracted from the current and adjacent (previously segmented) slices and therefore intrinsically robust to gray level and shape variations. In the third algorithm, a dynamical thresholding method which has a slice by slice manner and minimizes the weighted sum of false negative/positive errors is proposed. The developed algorithms give sufficient performance for different modalities, varying contrast, dissected liver regions and atypical liver shapes. Results indicate that we have effectively overcome the challenging difficulties explained before.

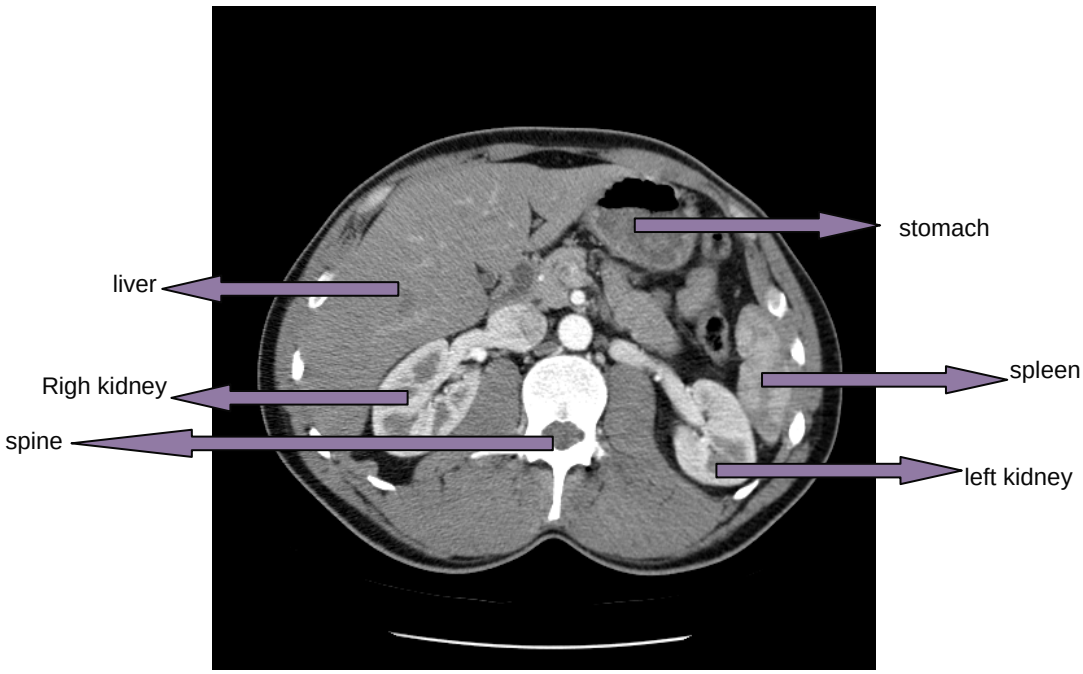
The rest of the thesis is organized as follows. The liver anatomy, liver surgery planning and procedure are presented in Chapter 2. Overview of abdominal organ segmentation and its challenges are introduced in Chapter 3. Proposed algorithms dealing with these challenges are explained in Chapter 4. Finally, conclusion and future plans for the improvement of the system are discussed in Chapter 5.

CHAPTER TWO
LIVER ANATOMY, LIVER SURGERY PLANNING AND PROCEDURE

2.1 Liver

The liver is an organ especially exists in vertebrates. It plays a fundamental role in metabolism and has various functions in the body, including glycogen storage, plasma protein synthesis, and drug detoxification. It lies below the diaphragm in the thoracic region of the abdomen. It produces bile, an alkaline compound which aids in digestion. It also performs and regulates a wide variety of high-volume biochemical reactions requiring specialized tissues.

The adult human liver normally weighs between 1.7 - 3.0 kilograms and it is a soft, pinkish-brown "boomerang shaped" organ. It is the second largest organ and the largest gland within the human body. It is located on the right side of the upper abdomen below the diaphragm as shown in Figure 2.1. The liver lies on the right of the stomach and makes a kind of bed for the gallbladder.



Figıre 2.1 Abdominal structures and location of the liver

2.2 Flow of Blood

The splenic vein, joins the inferior mesenteric vein, which then together join with the superior mesenteric vein to form the portal vein, bringing venous blood from the spleen, pancreas, small intestine, and large intestine, so that the liver can process the nutrients and byproducts of food digestion.

The hepatic veins drain directly into the inferior vena cava.

The hepatic artery is a blood vessel, which supplies the liver with oxygenated blood. It supplies 20% of the liver's blood.

Heptic portal vein is a blood vessel, which drains venous blood into the liver from the entire gastrointestinal tract. Approximately 60% to 80% of the blood flow to the liver is from the portal venous system.

2.3 Regeneration

The liver is among the few internal human organs capable of natural regeneration of lost tissue; as little as 25% of remaining liver can regenerate into a whole liver again.

2.4 Liver Surgery Planning and Donor evaluation

Live donor liver transplantation was first applied in 1989 to children in response to the severe scarcity of pediatric organ donors (Raia, Nery and Mies 1989; Broelsch, et al. 1990). The expansion of live donor liver transplantation to the adult population initially began in countries where the availability of cadaveric donors was scarce and in some cases totally unavailable (Lo, et al. 1996). Severe shortages of cadaveric organs along with the exponential growth in the number of patients have resulted in an increasing acceptance of live donor adult liver transplantation in Europe and the United States (Marcos, Ham, Fisher, Olzinski, Posner 2000; Malago, Burdelski, Broelsch 1999).

The donor selection is normally done in three phases. In the first phase, a potential donor is identified by obtaining demographic data and considering the relationship between the donor and the recipient. After explanation of the surgical procedure and description of the evaluation process a laboratory estimation of blood compatibility and normal screening is done. In the second phase, the anatomical conditions of the donor are clarified. For that reason CT images are acquired to observe different vessel systems (portal vein, liver vein, bilary duct and arteries) within the donor liver. With the help of these images the applicability and complexity of the surgical procedure is estimated. After the anatomical analysis a psychological estimation of the donor is performed. After the declarative statement of the laboratory, the radiologists and internists that the surgical intervention is possible for the donor the evaluation process gets into the third phase. In that last phase the recipient is re-evaluated to ensure that he has not become too sick for live donor liver transplantation

The process chain, especially the second phase, reflects one of the main problems in donor evaluation: the anatomical examination. The analysis of the vascular structures and a valid volumetric estimation of the donor graft size and the remaining liver tissue is a crucial step for surgery planning. However, only very experienced radiologists are able to verify the three dimensional structures of vessels. To close that gap in donor evaluation, liver segmentation is an essential step.

2.5 Liver Surgery Procedure

2.5.1 Liver Segmentation

Identification of the liver in medical images is mainly based on CT and/or MR image acquisition systems. Segmentation of liver is first step in building Computer Aided Diagnosis and Surgery Planning systems. Identification of liver and isolate it from its surroundings help track the liver during the surgery and avoid injury mistakes. It is helpful to use prior domain knowledge about abdominal area for identifying the liver. Purposes of liver segmentation can be categorized as:

- Decision support
- Resectability of liver
- Resection area
- Suitability as donor
- Spatial relations
- First step for determining borders of vascular territories
- Remaining functional liver parenchyma
- Volumetric estimations
- 3D rendering (visualization)
- Surgical planning

2.5.2 Vessel extraction and Couinaud's classification

The positions of large hepatic vessels are of great importance when planning liver surgery procedure. Surgeons and radiologists are typically base their evaluation on a visual inspection of the 2D slices produced by the different imaging modalities. However, it is difficult to figure out liver vessel structures from 2D images. Therefore, 3D rendering of identified structures and visualization of intrahepatic vessels is a valuable aid. After identification of vascular territories, Couinaud classification (Figure 2.2) of liver based on these territories is necessary to obtain further information about resection volume.

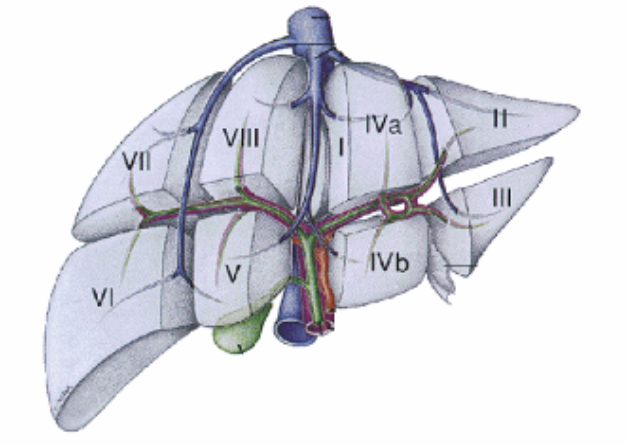


Figure 2.2 Couinaud Classification

2.5.3 Volume calculations

A preoperative and non-invasive estimate of the donor's liver volume is needed to be measured to ensure sufficient functional liver reserve for survival after surgery, and to obtain a graft of adequate volume to suit the recipient's features. In the recipient, the ratio between the graft size and the recipient's body weight preferably must be higher than 0.8%–1% (Kiuchi et al. 1999) or the ratio between the graft size and the standard liver volume (Urata et al.1995) must be higher than 50% (Kawasaki et al. 1998). In the donor, a remnant liver volume of 30% of the standard liver volume is usually considered to be the lower limit (Fan et al. 2000). Lower values are associated with higher morbidity and mortality in both the recipient and the donor due to the small-for-size syndrome.

2.5.4 Visualization

Segmentation of liver and vessel structures allows the creation of three-dimensional surface models for visualization of patient anatomy. The advantage of a surface model representation of anatomy is that it gives a three-dimensional view from any angle, which is an improvement over two-dimensional cross sections through the original grayscale data.

CHAPTER THREE
OVERVIEW OF ABDOMINAL ORGAN SEGMENTATION & ITS CHALLENGES

3.1 Identification Methods & Challenges

3.1.1 Manual Identification

Manual segmentation refers to the process whereby an expert segments and labels all slices in a set by hand. The manual method is believed to be more accurate. In addition, the use of an expert ensures that the segment boundaries and labels are perceptually valid. However, manual identification is a time consuming and tedious process. In addition, its results heavily depend on the skill of the user.

3.1.2 Automatic Identification

In automatic identification, several issues should be encountered. One of them is blurred and low contrast image which is resulted from partial volume effects, patient movement and beam hardening. Different organs/tissues may have similar gray levels. Same organ may exhibit different gray values in different cases and different image slices of the same case due to the administration of a contrast media and different machine setup. Anatomical structures of an organ in different image slices are different. Even for the same slice position, liver's shape may vary from patient to patient.

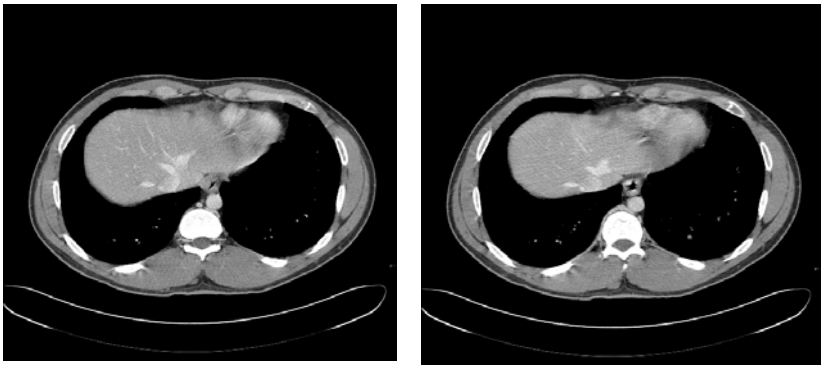


Figure 3.1 Partial Volume Effect

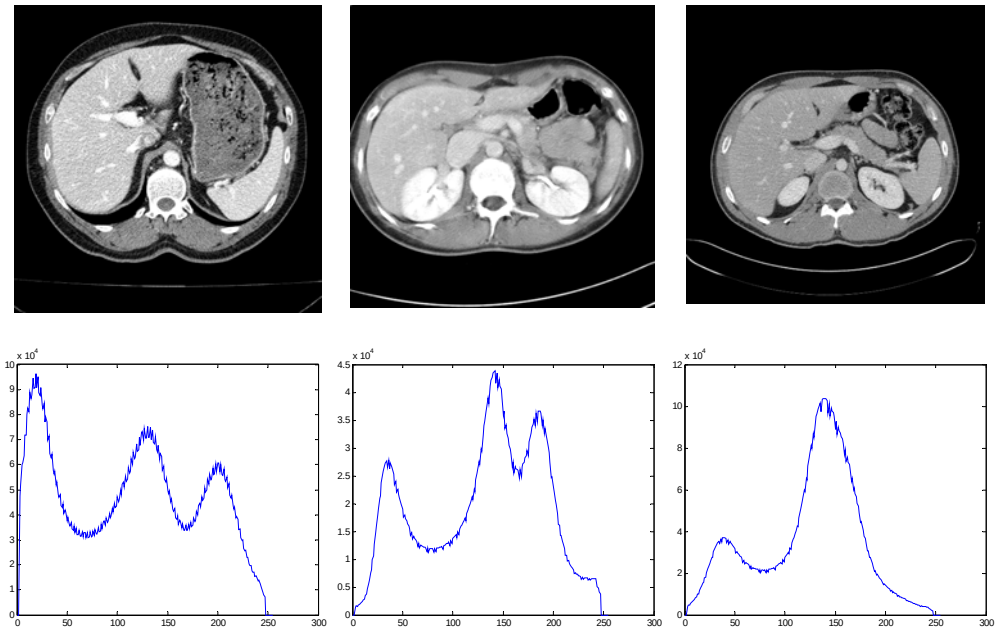


Figure 3.2 High Contrast vs. Low Contrast CT Images

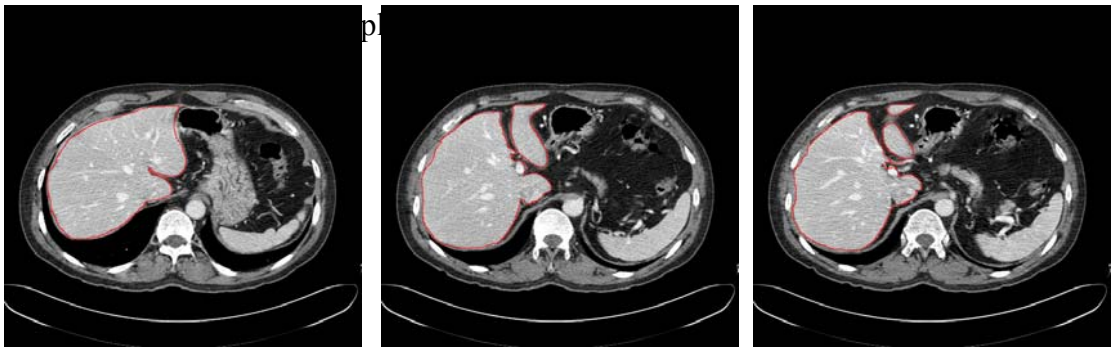


Figure 3.3 One and Multiple Component Liver

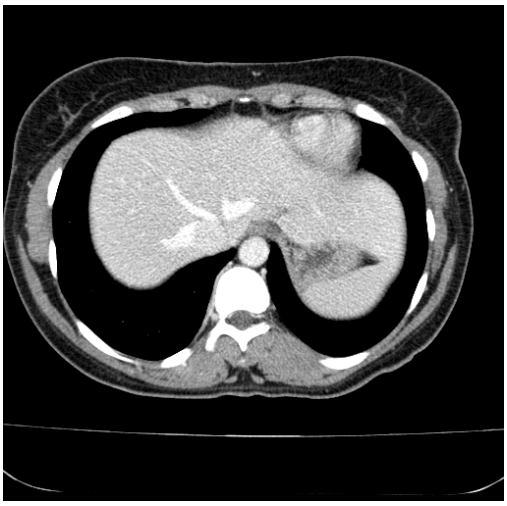


Figure 3.4 Liver and Spleen Interaction

3.2 Overview of Abdominal Organ Segmentation

Segmentation is perhaps the most crucial issue and the stumbling block in the effective use of 3D medical image volumes. Segmentation determines the size, shape, and position of objects in the volume. For example, to create 3D liver images, one may want to determine the size and shape of the liver, tumors, and blood vessels.

There are plenty of segmentation methods. Thresholding is the simplest and most common method. It assumes each type of tissue has a low and high threshold and tries to find these values.

Percentage classification (Ney, Fishman & Magid 1990) is a technique for 3D imaging. In the standard percentage classification model, each material is represented by four thresholds: LO, L100, H100, and HO. The percentage of a given material in a voxel is estimated by a piecewise linear function that is zero outside LO and HO, one between LlOO and H100, and a linear ramp elsewhere. Histogram-based classification is an extension of this technique in which the parameters of the percentage classifier are determined automatically.

Starting from some seed point, region growing (RG) (Acharya & Ray 2005) techniques segment images by incrementally recruiting pixels to a region based on some predefined criteria. Two important segmentation criteria are value similarity and spatial proximity. It is assumed that pixels that are close to each other and have similar intensity values are likely to belong to the same object. The main disadvantage of region growing approach is that it often requires user-supplied seed points. Due to the variations in image intensities and noise, region growing can result in holes and oversegmentation.

Edge based methods such as snakes (active contours) (Acharya et al. 2005) and livewire algorithm are also commonly used for organ segmentation. Active contours, developed by Kass et al, is a method of molding a closed contour to the boundary of an object in an image. The snake model is a controlled continuity closed contour that

deforms under the influence of internal forces, image forces, and external constraint forces. The internal contour forces provide a piecewise smoothness constraint. The image forces manipulate the contour toward image edges. The external forces are the result of the initial positioning of the contour by some a priori means.

Livewire (Barrett & Mortensen 1997) is a semi-automatic general purpose segmentation which finds the globally optimal path from the start node to a goal node by minimizing cumulative cost using Dijkstra's graph searching algorithm. The cost function is a weighted sum of the component cost functions calculated from the laplacian zero-crossing, the gradient magnitude and the gradient direction.

Mathematical morphological consists of applying basic set operations such as dilation, erosion, opening, closing and morphological reconstruction. It can be useful for the refinement of the object contours detected in the previous segmentation steps.

Pixel classification (Acharya et al. 2005) is a pixel to label transform. Derived image features that are able to distinguish between the pixels of different classes are used to classify pixels. Unsupervised or supervised classifiers such as multi layer perceptron networks (MLP), self organizing feature maps (SOFM), Bayesian classifier, etc. can be used dependent on the application.

Each method alone has drawbacks. There is currently no single segmentation method that yields acceptable results for every medical image.

CHAPTER FOUR
PROPOSED LIVER SEGMENTATION ALGORITHMS

Segmentation of liver from CT series prior to the liver transplantation operation is necessary for surgery planning. In clinical applications, segmentation of liver is generally performed manually. However, this procedure is not only time consuming but also heavily dependent on the user. To automatize this process, two algorithms are proposed. The first algorithm is time efficient and use k-means clustering as the classifier. The second and third ones are capable of dealing with atypical liver shapes (Figure 3.4) and use Multi Layer Perceptron network and a dynamical thresholding method. In the following, the details of these algorithms will be explained.

4.1 K-means Clustering Based Segmentation of Liver

Identifying liver region, calculation of the liver volume and determination of the vessel structure from abdominal Computed Tomography datasets is one of the essential steps in visualization prior to the hepatic surgery. Because of the high number of slices, manual segmentation of the liver is time consuming, tedious and depends on the experience. Moreover, due to several reasons automatic segmentation of the liver is a very difficult task. In this paper, we propose an algorithm that can handle the problems in automatic segmentation of the liver. Developed algorithm has three stages pre-processing, classification and post-processing and its performance is evaluated by area error rate which is applied to 20 datasets. The results show that, the proposed algorithm gives satisfactory results within a short span of time.

4.1.1 Patient Datasets

Our datasets were acquired after contrast agent injection at portal phase using a Philips Secura CT with 2 detectors and a Philips Mx8000 CT with 16 detectors, both equipped with the spiral CT option and located in Dokuz Eylül University Radiology Department. Spiral CT acquires data continuously, in a spiral path, as the patient is transported at a constant speed through the gantry. This technique scans the entire liver

in 15 to 30 seconds and offers several advantages for both liver tumor detection and 3D visualization. Its speed also reduces or eliminates respiratory misregistration between slices.

17 datasets (CT series), which were obtained by these scanners, consist of 12 bit DICOM images with a resolution of 512 x 512. The datasets were chosen randomly from the Picture Archiving and Communication System (PACS). All of the 17 CT series have 3 to 3.2mm slice thickness and this corresponds to a slice number around 90 (minimum 77, maximum 105 slices).

Our segmentation system is designed to work with 8 bit images to support all image types. Therefore, 12 bit DICOM images are reduced to 8 bit using window center and window width information, which are stored in Meta information header of the original DICOM images. Although a simple proportional scaling ([0, 4095] → [0, 255]) would be the most obvious way of such a conversion, windowing is used to reduce the undersampling effect. By using windowing, the full contrast of the output display range is expanded over actually useful part of the input density range (Bidaut, 2000).

4.1.2 Segmentation of the Liver

Proposed liver segmentation algorithm consists of three stages: pre-processing, classification and post-processing.

4.1.2.1 Pre-processing

It is observed that some datasets have three lobes in their volumetric histograms (Figure 4.1) where these lobes correspond to the fat tissue, darker soft tissues (i.e. muscles, stomach, intestines) and brighter soft tissues (i.e. heart, kidney, spleen) from left to right, respectively. The liver belongs to both second and third lobes with varying ratios. These datasets are called ‘high contrast’ because the gray level value of the liver is different from the adjacent tissues and organs. In ‘low contrast’ datasets, dark and bright soft tissues form only one lobe, thus the volumetric histograms have two lobes in total. In these datasets, it is harder to segment the liver because of the gray level similarity with adjacent organs. Therefore; the contrast of datasets having two lobes are

enhanced via histogram specification (Masumoto et al., 2003) process which forces it to have three lobes (Figure 4.2).

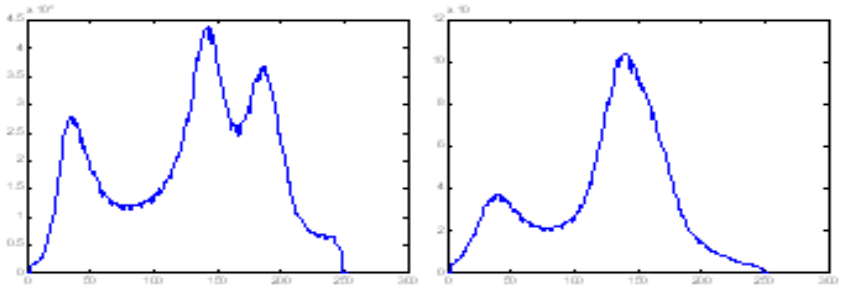


Figure 4.1 Multi-modal and bimodal volumetric histograms representing high and low contrast CT series

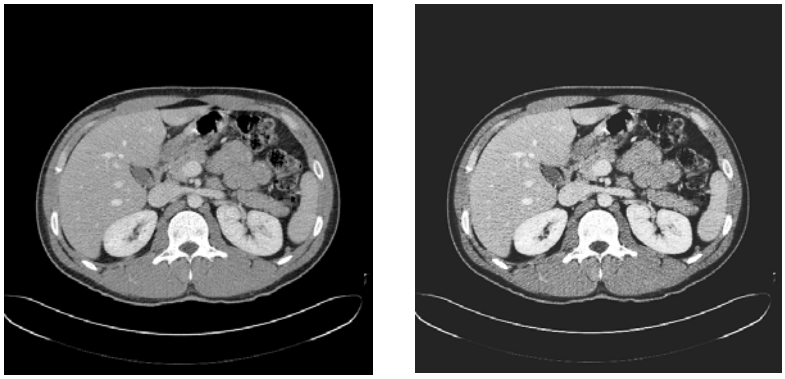


Figure 4.2 Result of Histogram Specification Process

In order to determine the lobe number; first the volume histogram (Figure 4.3) is smoothed (Figure 4.3) via a moving average filter. Then using the gradient of the smoothed histogram (Figure 4.3), zero-crossings from positive to negative values are determined in order to obtain peak locations of volume histogram. Number of corresponding peaks gives number of lobes.

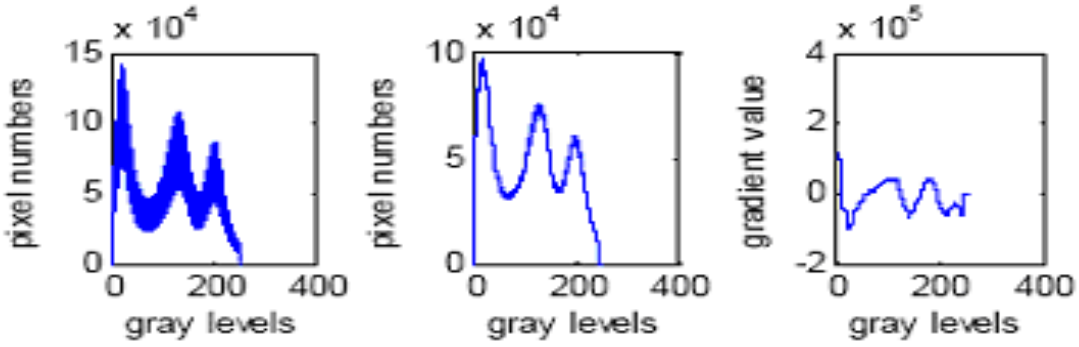


Figure 4.3 Volumetric Histogram, Smoothed Volumetric Histogram and Gradient of Smoothed Histogram

4.1.2.2 Classification of the Liver

Images obtained after pre-processing stage are classified to five clusters using K-means algorithm. K-means algorithm (MacQueen, 1967) partitions the pixels in the image into n clusters by using an iterative procedure. The aim is to minimize the sum, over all clusters, of the within-cluster sums of gray level value-to-cluster centers:

$$J = \sum_{j=1}^{k} \sum_{i=1}^{n} \left\| x_i^{(j)} - c_j \right\|^2$$

where $\| x_i^{(j)} - c_j \|^2$ is a chosen distance measure between a gray level value $x_i^{(j)}$ and the cluster center c_j is an indicator of the distance of the *n* data points from their respective cluster centers. In our system, Euclidean distance metric and batch update method (Haykin, 1998) are used where every iteration consists of reassigning gray level values to their nearest cluster centers, all at once, followed by recalculation of cluster centers.

The performance of K-means algorithm is dependent to the initial cluster centers. Therefore, determining initial cluster centers to get acceptable results is important. Two of the initial centers of the clusters are chosen to be 30 (for the background), 255 (for the spine and the ribs). Third initial cluster center is chosen the first valley of the volume histogram which is obtained by determining the first zero-crossing from negative to positive value (generally around 80). The remaining ones are two equidistant gray level values between 255 and the third cluster center. In Figure 4.4, the result of K-means algorithm is shown.



Figure 4.4 Five Clusters After K-mean Clustering

4.1.2.3 Post-processing

After separating the cluster belonging liver, it can be observed that there is also various non-liver tissues as shown in Figure 4.5. In order to remove these non-liver tissues, a post-processing stage is applied. In this stage, morphological filling process is applied to remove black spots appear inside the liver. After that, weak connections between liver and adjacent organs are broken via morphological erosion. Its mathematical expression is shown in equation where A denotes clustered image and B denotes structuring element (Masumoto et al., 2003).

$$A \odot B = \left\{ x \middle| (\hat{B})_x \subseteq A \right\}$$

To identify the pixels belonging the liver, an iterative slice-by-slice procedure is applied. First of all, an initial image where liver is the biggest organ is selected to segment liver (there are about 15-20 slices in a dataset having 90 slices which satisfies that condition). Initial image segmentation is completed after the selection of the biggest connected component. Proposed algorithm segments other slices from initial image toward the last and beginning image. There is a bit change in shape and size of liver between two adjacent slices. Therefore, the search region for current slice is reduced by just focusing the region which is enlarged of previous segmented slice. In the post-processing stage, reducing the search region provides less

computational complexity while increasing performance. The biggest connected component in the search region is liver, so the pixels belonging liver can be determined easily. Finally, to eliminate the effect of previously applied erosion, the morphological dilation shown in equation is applied (Masumoto et al., 2003).

$$A \oplus B = \left\{ x \left| (\hat{B})_x \cap A \neq \varnothing \right. \right\}$$

The result of post-process is shown in Figure 4.5.

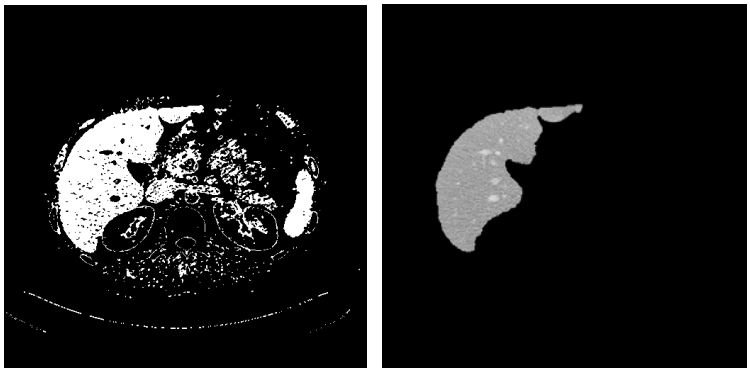


Figure 4.5 Result of Classification and Post-processing

4.1.3 Evaluation

The segmentation results are evaluated by using the area error rate (AER) (Seo et al., 2004). AER is defined as the area difference between the region segmented by the algorithm (RA) and the region segmented manually (RM). Defining a union region RU as RA∪RM and an intersection region RI as RA∩RM, AER is equal to:

$$AER = \frac{RU - RI}{RM} \times 100\%$$

In our evaluation, AER is calculated directly (without any boundary modification) between the manually and automatically segmented images. The manually segmented images are segmented by an expert radiologist from Dokuz Eylül University (DEU) Radiology department.

The slice-by-slice average AER for 20 datasets with the K-means algorithm is shown in Figure 4.6. It is observed that the algorithm shows better performance for the slices at the middle and at the end of the datasets. The high AER values for the slices at the beginning of the datasets are due to unclear boundary between the heart

and the liver. The average AER for the complete dataset is calculated as 14.88%. Figure 4.7 shows the average AER for each patient dataset.

As mentioned above, the main points where the K-means algorithm fail are the first slices where the heart and the liver can hardly be segmented even with the human eye, the patient datasets with atypical liver shapes and the separation of the tissues in 'low contrast' dataset where the gray level value of the adjacent tissue (organ or vessel) is very close to the liver.

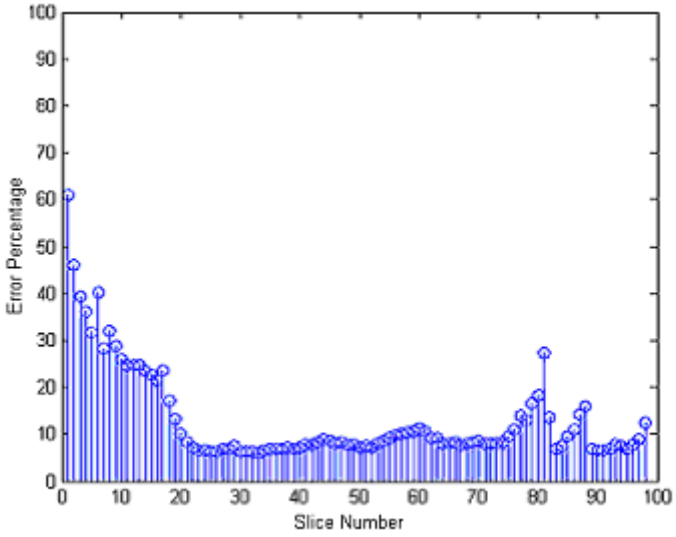


Figure 4.6 Average AER for each slice number

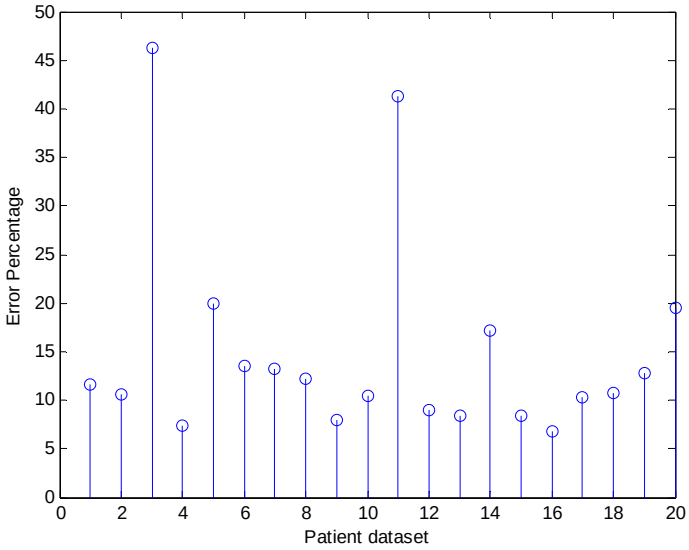


Figure 4.7 AER for CT series

4.2 Patient Oriented and Robust Semi-Automatic Liver Segmentation using Multi Layer Perceptron

In order to segment liver, a three stage; semi-automatic liver segmentation algorithm that adapts its parameters according to each patient by learning the dataset characteristics in parallel to segmentation process is proposed. At the first stage (pre-processing), the pixels which certainly do not belong to liver are excluded. At the second stage, multi layer perceptron is used to classify the pixels as belonging to liver or other tissues, depending on the image characteristics. At the final stage, the segmentation performance is increased with a post-processing. The segmentation results are evaluated by using area error rate and volume calculations. The results show that, the proposed algorithm gives better results especially for atypical liver shapes and low contrast studies where several algorithms fail.

4.2.1 Patient Datasets

The datasets were acquired as described section 4.1.1. 20 patient datasets are divided into two groups based on their volumetric histograms, namely ‘high contrast’ and ‘low contrast’ as described section 4.1.2.1. In 20 patient datasets, it is found that 15 datasets belong to ‘high contrast’ group while 5 datasets belong to ‘low contrast group. The developed algorithm first determines the group of the dataset and applies different pre-processing and post-processing methods based on this decision.

4.2.2 Segmentation of the Liver

The developed segmentation algorithm is designed to have three stages. The first stage is preprocessing which consists of the removal of the irrelevant tissues (the fat tissue, the spine, the right kidney and the ribs) from the original images and finding the smallest possible region of interest (ROI), where the liver tissue is known to exist.

Before starting the process, the user selects a slice which is called ‘initial kidney image’. The ‘initial kidney image’ is the slice where the liver and the right kidney exist together for the last time in the dataset. Starting from this image, the algorithm for removing the right kidney runs through the dataset until the right kidney disappears in all slices.

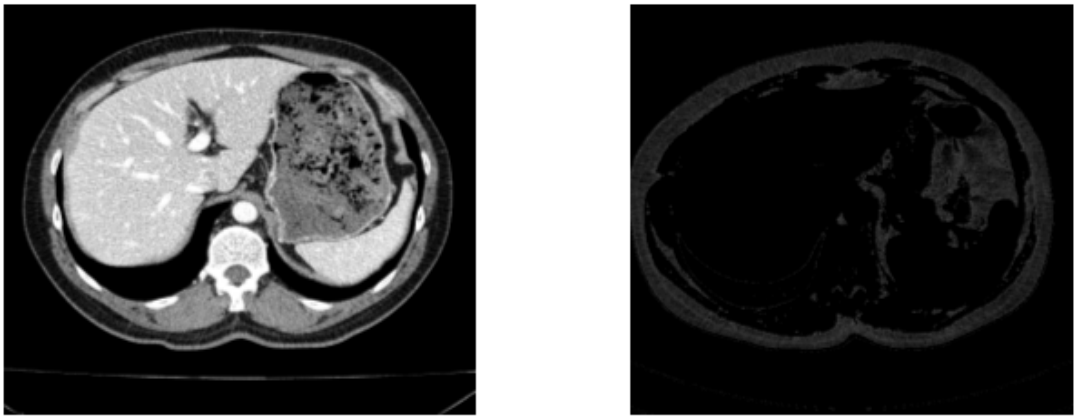
In the proposed algorithm, selection of ‘initial kidney image’ is the only interface with the user. Needless to say, this is a rather simple task for the user.

4.2.2.1 Pre-processing

After the selection of the ‘initial kidney image’, the pre-processing starts by removing irrelevant tissues and organs including the fat tissue, the spine, the ribs and the right kidney.

4.2.2.1.1 Removing the Fat Tissue. To remove the fat tissue from a patient dataset that consists of several CT images (Figure 4.8 a), an adaptive thresholding method has been applied. In the volumetric histogram of a CT series, the first lobe of the histogram corresponds to the fat tissue if there is enough fat tissue in the patient. To locate this lobe valleys of the histogram have to be found. For this reason, an averaging filter is applied to eliminate high frequency components of the histogram. Then the gradient of the smoothed histogram is calculated and valleys are found where the gradient histogram changes from negative to positive. Finally, a proper threshold value is found as the gray level value of the first valley. The tissues, which are removed with the application of the determined threshold value, are shown in Figure 4.8 b.

In young or/and fit patients, the fat tissue might be so less that it does not correspond to a lobe in the volumetric histogram. To prevent wrong determination of the threshold value in these datasets, the maximum gray level value for the fat tissue threshold is limited to 100.



(a) (b)

Figure 4.8 a) Original Abdominal Image and b) Thresholded Fat Tissue

4.2.2.1.2 Removing the Spine and the Ribs. The common method to remove the spine and the ribs is thresholding because of their high Hounsfield values. In the developed method, thresholding is combined with anatomy knowledge to remove the spine and the ribs.

First, an empirically determined threshold value (T=245) has been applied to the image (Figure 4.9 a) to remove fat, skin and muscle tissues. The resulting image consists of the spine, the ribs and contrast enhanced tissues (i.e. liver vessels, kidneys) (Figure 4.9 b). Since it is known that the spine and the ribs surround the contrast enhanced tissues, a topology based method is used to segment them. First, the row and column projections are calculated from the thresholded image. The column projection is used to find the columns where the ribs start (from left and right) by using the first and last non-zero values on it. The row projection is used to determine the row where the spine and ribs start (from the bottom) by using the first non-zero value on it. The middle point of the corresponding row and the values determined as the starting point of the ribs are then used to make a frame as shown in Figure 4.9 b. By dilating this frame, the ribs and the spine are excluded (Figure 4.9 c). To segment the spine and the ribs by combining these two images, binary morphological image reconstruction (BIMIR) (Vincent, 1993) is used.

Intersecting framed image and the thresholded image by using ‘AND’ operation, the marker image is generated. Using the thresholded image as the mask in the BIMIR, the spine and the ribs are obtained (Figure 4.9 d). The advantage of using BIMIR is that it is possible to reconstruct of a rib correctly even if some parts of it remain outside the frame as in(Figure 4.9 c).

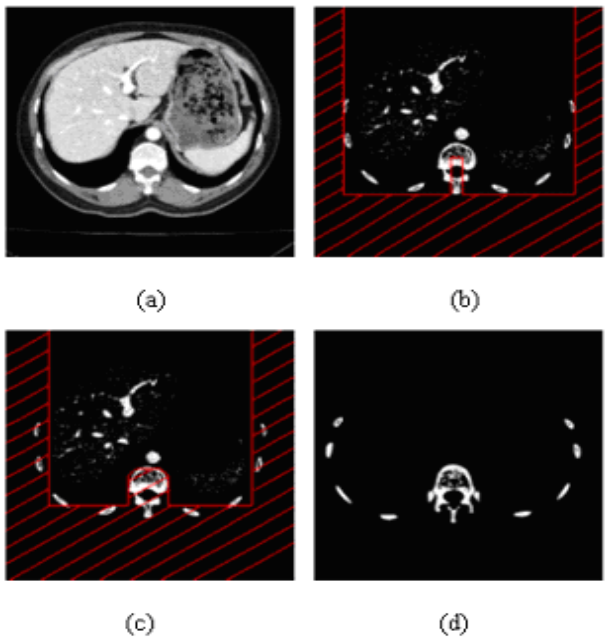
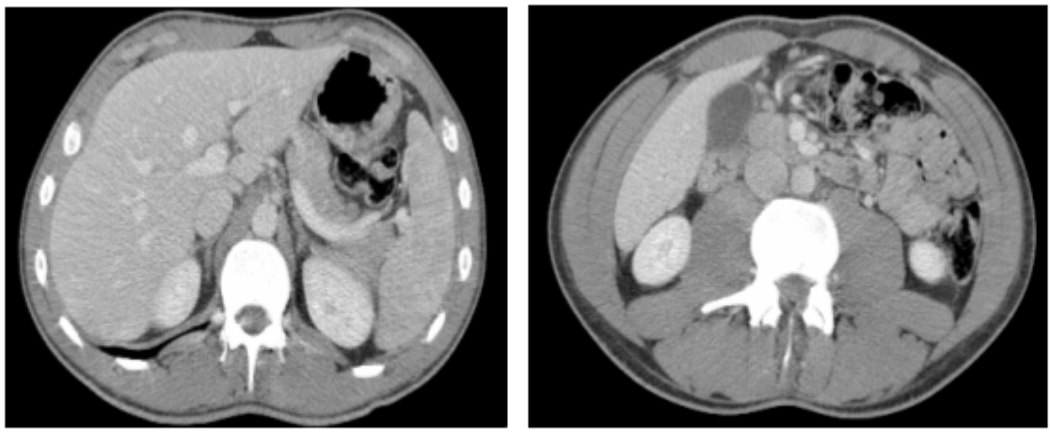


Figure 4.9 Removing the spine and the ribs

4.2.2.1.3 Removing the Right Kidney. The right kidney is an adjacent organ to the liver which can have different gray level values due to the contrast media (Figure 4.10). Moreover, its shape and location differs from patient to patient. Also the shape of the kidney varies through the slices of a CT series (Figure 4.10). Because of the partial volume affect and injection of contrast media, sometimes the border between the right kidney and the liver almost vanishes. Therefore, the elimination of the kidney should be done prior to the segmentation of the liver to increase segmentation performance.

After removing the ribs and the spine, the detection of the right kidney starts from the ‘initial kidney image’, which is the slice where the liver and the right kidney exist together for the last time in a dataset (Figure 4.10 b). This user selected slice is mostly the last slice for a CT series, however sometimes the kidney ends before the

liver. Kidney detection process starts from ‘initial kidney image’ and continues through the beginning of the series until the right kidney is removed from the dataset. The reason for the direction of the process is the gray level value similarity and unclear boundary between the liver and the right kidney at the slices, where the right kidney begins to appear. In such images, the liver and the right kidney could not be separated even by complicated methods. The only way to segment the kidney in those conditions is to use the information obtained from a slice where the liver and the right kidney can be separated easier (Figure 4.10 b).



(a) (b)

Figure 4.10 The right kidney and the liver (a) at the preceding slices where they can not be separated easily, (b) at the succeeding slices where the border between them is more clear.

The removal of the right kidney starts with the classification of the ‘initial kidney image’ into 5 clusters by using the K-means algorithm. The initial centers of the clusters are chosen to be 30 (for the background), 255 (for the spine and the ribs), threshold found for the fat tissue (generally around 80) and two equidistant gray level values between 255 and the threshold found for the fat tissue. After the application of the k-means method, it is observed that the kidneys are always assigned to the brightest cluster together with the spine and other very bright tissues (Figure 4.11 top right).

Then, a search region is generated at the right of the spine, which is based on the location of the spine (Figure 4.11 top left). The search region is determined at a

location, where at least some part of the kidney is most likely to exist, by using anatomical information.

To segment the kidney from this result, BIMIR is used. In the ‘initial kidney image’ the marker is the seed region and the mask is the image that consists of pixels which belong to the brightest cluster The largest connected component after the BIMIR operation forms the kidney (Figure 4.11-Output Image).

The kidneys at the other slices are then detected iteratively. For each preceding slice, the skeleton of the previously segmented kidney is used as the new marker image. And the image of the pixels that belong to the brightest cluster of the current slice is used as the mask image. Using BIMIR algorithm gives the kidney structure of the current slice. This procedure is illustrated in Figure 4.11.

The skeleton of a kidney is calculated using iterative skeletonization (thinning), which is a method to reduce all objects in an image to lines, without changing the essential structure of the image (Blum, 1967). It removes the pixels on the boundaries of the objects but does not allow objects to break apart. The pixels remaining make up the image skeleton.

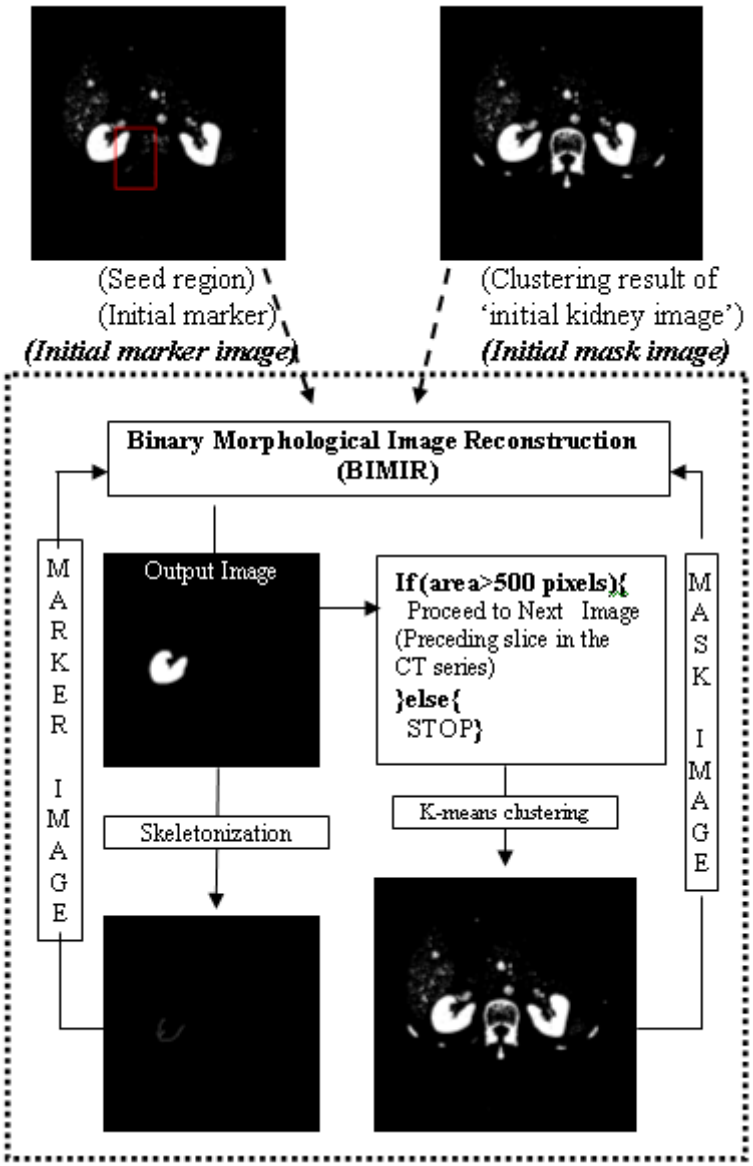


Figure 4.11 Determination of the kidney

Since the skeleton of the previously segmented kidney can be thought as an iteratively eroded image, BIMIR restore exactly the shape of the kidney in the current slice without depending on the similarity between the shapes and the structuring element. By using skeletonization combined with BIMIR; kidneys are detected automatically until the kidney area drops to a user defined value (default=500 pixels).

4.2.2.1.4 ROI Selection. For reducing the computation complexity and for increasing the performance of the segmentation algorithm, as much irrelevant information as possible should be removed from the image at the preprocessing. From the anatomy knowledge, we know that the liver is surrounded by the ribs from the left, right and bottom, thus the pixels at the outer side of the ribs can be removed. Also the unnecessary parts from the top (starting from the first non-zero pixel) can be removed. The remaining ROI decreases the image size by 40% in average and reduces the computational complexity significantly.

4.2.2.2 Classification of the Liver

The second step of the segmentation procedure is the segmentation of the liver. This step consists of two parts:

1. Automatic selection and segmentation of an 'initial image'
2. The segmentation of the remaining slices one by one starting from the 'initial image'.

The 'initial image' is a slice where the liver boundary does not overlap with any adjacent organ boundaries, especially the heart and the right kidney. It is selected automatically by choosing the slice that comes just before the first appearance of the right kidney which is determined during the kidney removal stage. After the preprocessing stage, the segmentation algorithm starts from this 'initial image' and then runs through the end of the dataset. Then again starting from the 'initial image' again, it runs through the beginning of the dataset to complete the segmentation process.

After the segmentation of the initial image, liver structures at other slices are segmented iteratively. This iterative segmentation is done by using a multi layer perceptron (MLP).

It is worth to point that, the result of classification process gives rough results and these results are refined at the postprocessing stage (i.e. removal of the small mis-

segmented objects, identification of all components of the liver when the liver dissects into two or more regions).

4.2.2.2.1 Initial Image Segmentation. As previously mentioned, 'initial image' is a slice that should satisfy three constraints. First of all, the liver should have a relatively big area in the slice but it does not have to be the biggest organ. Second, it should consist of one connected component and third, the liver boundary should not overlap with any adjacent organs, (i.e. the heart and the right kidney). An example of an initial image is given in Figure 4.9.a. After preprocessing (Figure 4.12 a), the image can be classified into three clusters: background, bright organs and dark organs. Excluding the background pixels from the process, the two clusters are found using the Otsu's method (Otsu, 1979) by finding the optimal threshold to separate dark organs (stomach and muscle) and brighter organs (liver, spleen, and heart).

Otsu's method chooses the threshold value k that maximizes the between-class variance σ^2_B which is defined as:

$$\sigma^2_B = w_0.(\mu_0-\mu_T)^2 + w_1.(\mu_1-\mu_T)^2$$

where

$$w_0 = \sum_{q=0}^{k-1} p_q(r_q),\ w_1 = \sum_{q=k}^{255} p_q(r_q),\ \mu_T = \sum_{q=0}^{255} q.p_q(r_q),\ \mu_0 = \sum_{q=0}^{k-1} q.p_q(r_q)/w_0, \text{ and}$$

$$\mu_1 = \sum_{q=k}^{255} q.p_q(r_q)/w_1$$

Here $p_q(r_q)$ is the discrete probability density function, as in $p_q(r_q)=n_q/n$ where n is the total number of pixels in the image, and n_q is the number of pixels that have intensity level r_q (q=0,1,…,255).

Selecting the cluster which has the foreground organs (i.e. the right side of the threshold) (Figure 4.12 b) and then taking the biggest connected component in the slice results with the segmented liver structure (Figure 4.12 c).



(a) (b) (c)

Figure 4.12 Initial image segmentation (a) The preprocessed ‘initial image’ (b) Clustering result (c) The biggest component in the slice

4.2.2.2.2 Segmentation with Multi Layer Perceptron (MLP). After segmenting the initial image, the algorithm first runs downwards to the last slice and then upwards to the first slice starting from the initial image.

It is clear that the preprocessed images contain the liver, the tissues and the organs that have similar or darker gray level values than those of the liver because the brighter tissues and organs are removed at the preprocessing phase (except the bright tissues inside the liver). In order to discriminate these structures a feature based segmentation process is developed by using a Multi Layer Perceptron (MLP) as the classifier. The overall structure of the segmentation process using MLP is shown in Figure 4.13.

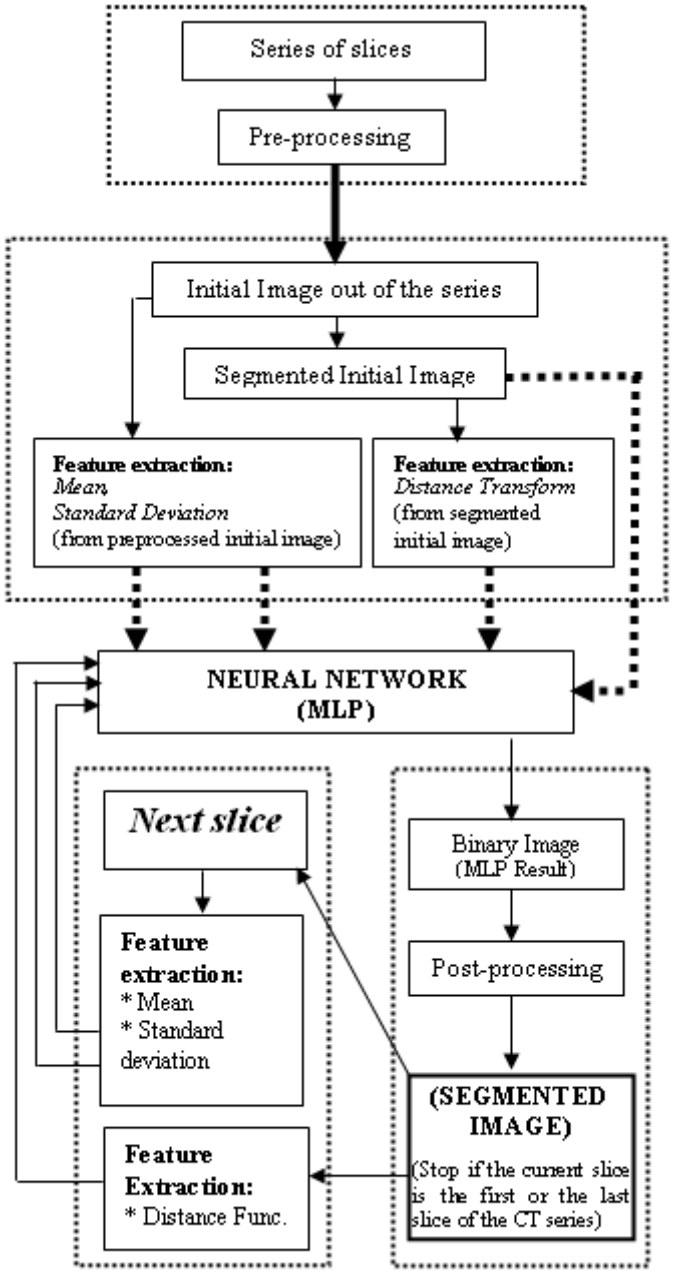


Figure 4.13 Segmentation process by using MLP

In segmentation with the MLP, the preprocessed 'initial image' and the segmented 'initial image' are used for initial training of the network. From the preprocessed 'initial image', two features (Mean and standard deviation) are calculated. Then, the distance transform is applied to the segmented 'initial image' and the pixel values after the transform are taken as an additional (third) feature. The features are calculated in a window of size 9x9 centered for a given pixel.

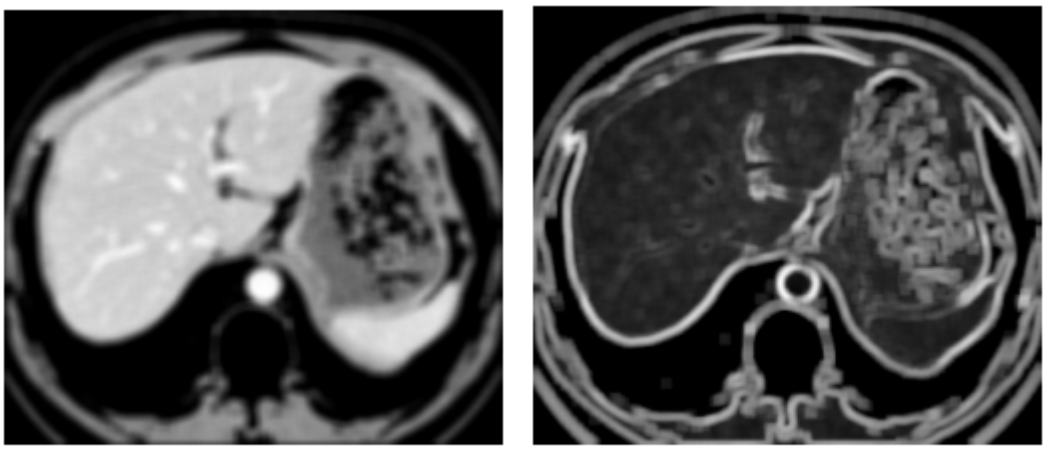
To represent the homogeneous regions (i.e. Liver parenchyma) in the current slice, we use the mean feature (Figure 4.14 a). For a pixel the mean gray level value is calculated by

$$\bar{x}_{ij} = \frac{1}{N} \times \sum_{i-4}^{i+4} \sum_{j-4}^{j+4} x_{ij}$$

To represent the edges (i.e. liver boundary) we use the standard deviation feature (Figure 4.14 b) which is calculated as:

$$\sigma_{ij} = \sqrt{\frac{1}{N} \times \sum_{i-4}^{i+4} \sum_{j-4}^{j+4} \left(x_{ij} - \bar{x}_{ij} \right)^2}$$

where $\bar{x}_{ij}$ is the mean value of the pixel x located at the position i, j and σ_{ij} is the standard deviation of the pixel located at the same position. N is the total number of pixels in the window which is equal to 81 in our approach.



(a) (b)

Figure 4.14 Feature images (a) mean (b) standard deviation

Finally, the distance transform feature is used to represent the previously segmented image. The distance transform provides a metric that measures the separation of the pixels in the image. The metric is calculated to measure the total Euclidean distance along the horizontal, vertical, and diagonal directions (Figure 4.15 a).

In our algorithm, the distance transform gives information about the liver location at the adjacent slice. Since the liver size and location does not change dramatically between adjacent slices, the distance transform of a segmented liver (Figure 4.15 b) gives quite important information about the liver shape and location at the adjacent slice.

2.8	2.2	2	2.2	2.8
2.2	1.4	1	1.4	2.2
2	1	0	1	2
2.2	1.4	1	1.4	2.2
2.8	2.2	2	2.2	2.8

(a)



(b)

Figure 4.15 Distance transform process (a) Distance transform of a binary image in which only the pixel at the center has value 1 (b) Distance transform of a segmented slice.

After the feature extraction, the network is trained initially by using the segmented initial image as the desired output and the calculated three features as the training data. At the network output, each input pixel is classified as belonging to the liver region or lying outside the liver region on the basis of these features.

After this initial training, weights are updated and iteration proceeds to the next slice. Mean and standard deviation features are calculated for the preprocessed next slice (which is the current slice to be segmented) and the distance transform is calculated from the previously segmented image. By using these features and the adjusted weights, the current slice is segmented. After the segmentation of the current slice, the network is trained again by using the features (calculated for the preprocessed and segmented images of current slice) as the input and the new segmented image as the desired output. After updating the weights, the algorithm proceeds with the next slice and this iterative procedure continues until all images are

processed. Using the previously adjusted weights as the initial weights of the next training phase, the training time is reduced significantly.

The MLP structure used for the segmentation consists of 3 neurons at the input layer, which corresponds to the number of input features. There are 8 neurons at the hidden layer. The weights are updated with backpropagation algorithm (MacQueen, 1967). The output layer consists of l neuron. The output of the network lies between 0 and 1 for each pixel and it is thresholded by 0.5. Then, for an input region belonging to the liver class, the output is designed to be unity whereas for all other the output is designed to be zero.

This network structure is determined to be the optimum after extensive experimentation and due to a compromise between efficiency and reliability.

4.2.2.3 Post-processing

The results obtained from the segmentation algorithms are roughly segmented liver structures (Figure 4.16). To remove small mis-segmented objects and for boundary refinement, a post-processing stage is needed. Moreover, identification of all components of the liver when the liver dissects into two or more regions is also done at the post-processing stage.

Post processing is handled differently for the slices before and after the “initial image” slice because of the different image characteristics.

In the post-processing phase of the slices after the ‘initial image’, a series of nonlinear filtering and morphological operations is applied to separate weakly connected components in the clustered binary image. First, a median filter is applied to remove the white spots appear at the background and black spots appear inside the liver. Then, erosion operation is applied to eliminate the small unconnected objects that do not sit within the structuring element. Next the skeleton of the previously segmented liver is obtained using skeletonization. By using BIMIR, in which the skeleton is used as the marker image and MLP result as the mask image, the liver is

identified. Usage of skeletonization also provides the important information about the separated parts of the liver when it dissects into two or more regions. The algorithm searches for the second and the third components automatically for the slices after the 'initial image'. After that, dilation operation is applied to restore the contours that have not been completely removed by the erosion.

The difference between post processing of the slices before and after the initial image is due to the existence of heart tissue in the slices before the initial image. For the slices before the initial image, the liver area from the previously segmented slice is not dilated because the heart can also be included due to gray level similarity of it with the liver. Another difference is that the algorithm looks for only one connected component for the first slices.

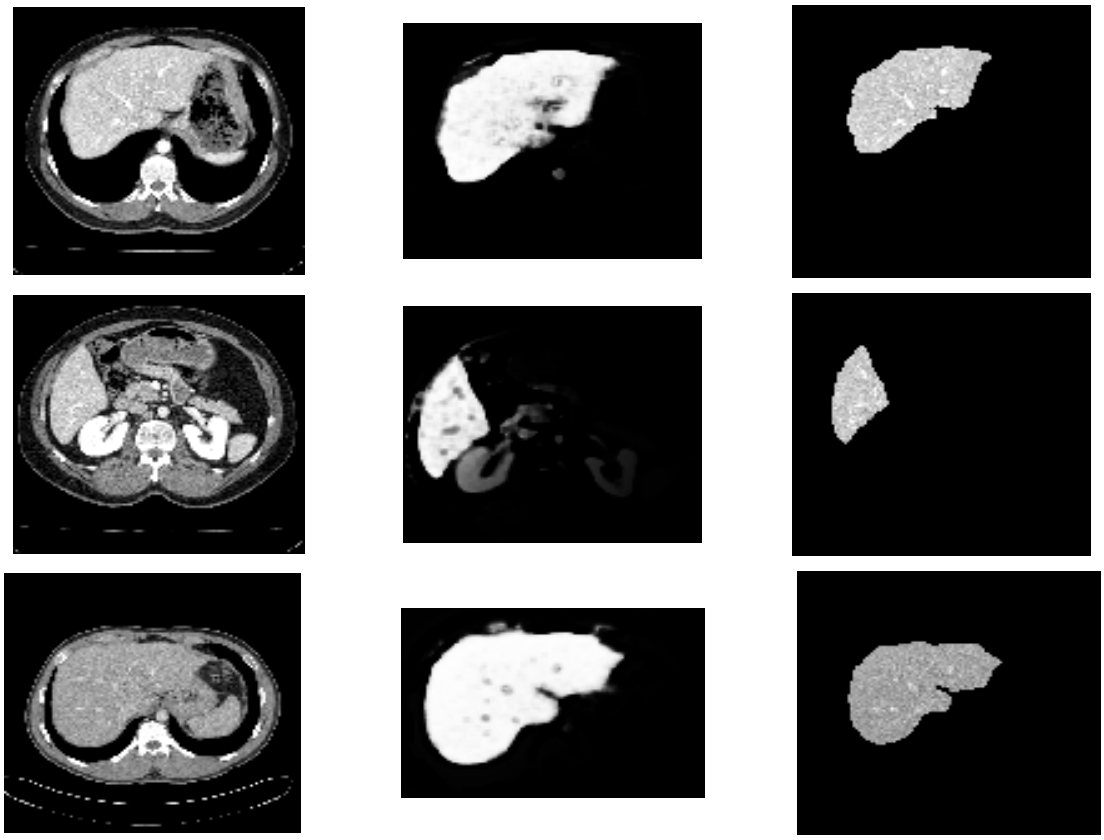
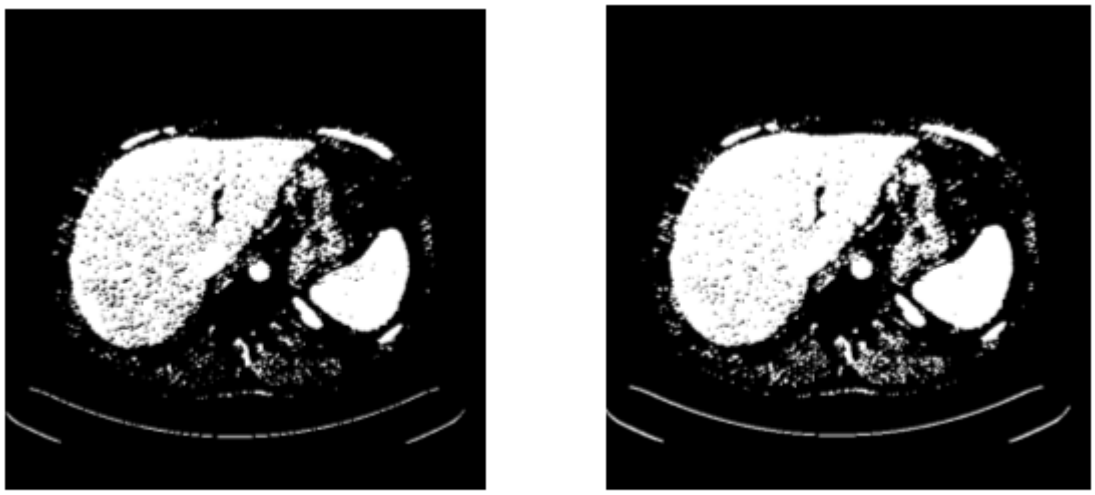


Figure 4.16 Result after classification and post-processing stages

Post processing is handled differently also for the low and high contrast datasets. In low contrast datasets, nonlinear filtering is applied in a different way such that the

value after the median is taken instead of the median value. This kind of filtering increases the connectivity of the liver by eliminating more dark spots than median filtering (Figure 4.17).



(a) (b)

Figure 4.17 (a) Affect of median filtering (b) affect of modified nonlinear filtering

4.2.3 Evaluation

The segmentation results are evaluated by using the area error rate (AER) as described in chapter 6.1.3. The slice-by-slice average AER for 20 datasets with the MLP algorithm is shown in Figure 4.18. It is observed that the algorithm shows better performance in the first slices where the heart and the liver can hardly be segmented even with the human eye, the patient datasets with atypical liver shapes and the separation of the tissues in 'low contrast' dataset where the gray level value of the adjacent tissue is very close to the liver. The average AER for the complete dataset is calculated as 12.32%. Figure 4.19 shows the average AER for each patient dataset.

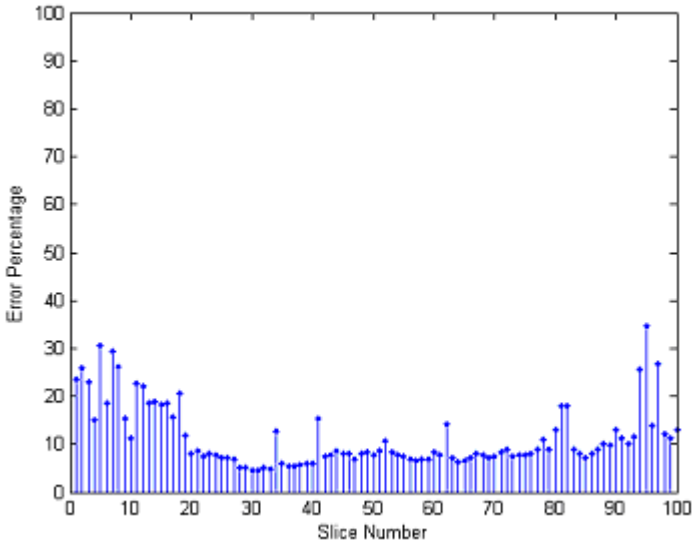


Figure 4.18 Average AER for each slice number

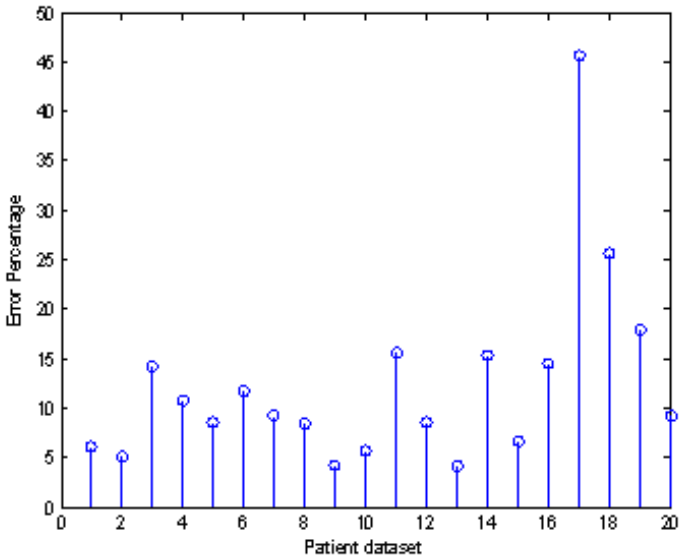


Figure 4.19 AER for CT series

4.3 Proposed Dynamical Thresholding Based Liver Segmentation

In this thesis, two algorithms were proposed in order to segment liver from CT series automatically. The first algorithm is time efficient but doesn't work for atypical liver shapes. The second one is capable of dealing with atypical liver shapes but time consuming. A third algorithm which is not only time efficient but also able to deal with atypical liver shapes is proposed. This algorithm uses a dynamical thresholding. Recently in (Gao L., Heath D.G., Kuszky B.S. & Fishman E.K. 1996) and (Lim S.J., Jeong Y.Y. & Ho Y.S. 2006), dynamical thresholding is used to help segmentation process. In (Gao L., Heath D.G. et al 1996), the peak of the histogram corresponding to the liver is determined and then upper and lower threshold values are determined by two offsets from the peak based on an empirical standard deviation of the gray level of the liver. In (Lim S.J. et al 2006), they consider a priori knowledge of the liver on abdominal CT images, such as shape and location in order to determine a ROI region, and then the threshold values are determined from pre-analyzed statistical information (such as average intensity distribution of the liver and muscle) of this localized region. However abdominal CT images has a very changeable contrast resulting variety of histogram. Also the shape and location of liver have significant differences from patient to patient. Therefore, shape and location based assumptions are not trustable. Furthermore, global or local histogram based thresholding do not guarantee the reasonable threshold values for further processes. Our strategy for overcoming these difficulties involves a dynamical thresholding method which has a slice by slice manner and minimizes the weighted sum of false negative/positive errors. In the following, the details of this algorithm will be explained.

4.3.1 Pre-processing

In the pre-processing stage, the ribs, spine and right kidney which are brighter tissues than liver are removed as described in chapter 4.2.2.1. This process allows liver to be

segmented only by one threshold. In addition, contrast of the datasets are determined either being low or high. Datasets having low contrast are enhanced via histogram specification process (Masumoto et al., 2003) as described in chapter 4.1.2.1.

4.3.2 Dynamical Thresholding

First of all, an initial image is segmented as described in chapter 4.2.2.2.1. Then, this segmented image is used to find an optimal threshold for that slice and this threshold updates itself in parallel to the segmentation process. This process is called dynamical thresholding which has a slice by slice manner and minimizes the weighted sum of false negative/positive errors;

$$\min_{T}(E) = w_1 \times FN + w_2 \times FP$$

where w_1 and w_2 are the weights, T is threshold, FN and FP are false negative and false positive errors. FN error represents the pixel numbers which are liver but detected as non-liver after dynamical thresholding method. FP error represents the pixel numbers which are not liver but detected as liver after dynamical thresholding method. In the applications, w_1 and w_2 are empirically chosen to be 0.7 and 0.3, respectively. The weight for FN error is chosen to be greater since it is more important not to label a pixel belonging to the liver as non-liver (FN) than to label a non-liver pixel as liver (FP). Because the effect of FPs can be compensated at post-processing stage while this is not possible for FNs.

The process is explained in Figure 4.20.

4.3.3 Post-processing

After dynamical thresholding, it can be observed that there is also various non-liver tissues. In order to remove these non-liver tissues, a post-processing stage is applied. In this stage, this post-processing stage is as described in 4.1.2.3. Additionally, a constraint for sudden and large region area change between adjacent slices is added. This constraint checks if the liver area expands dramatically between adjacent slices or not. This control is done by dilating the previously segmented liver with a 10x10 disc shaped structuring element. Then the difference between the

currently and the previously (dilated) segmented liver is obtained. If difference shows that the current segmentation result is greater than the dilated previous segmentation result, then the current segmentation result is limited to the dilated region. Although this operation does not prevent mis-segmentation for the current slice, it preserves the reliability of the process for succeeding slices.

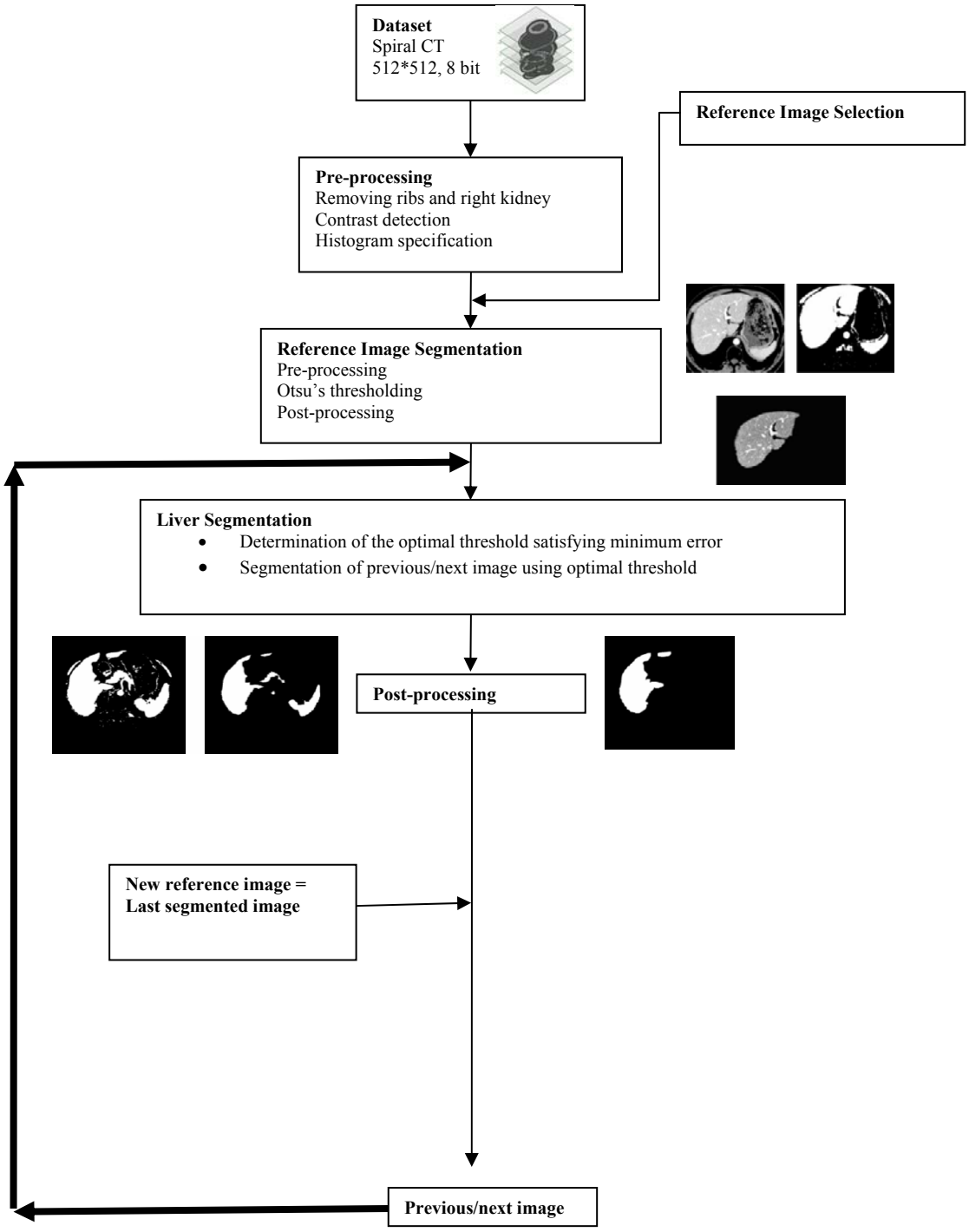


Figure 4.20 Dynamical Thresholding Process

4.3.4 Evaluation

The segmentation results are evaluated by using the area error rate (AER) as described in chapter 4.1.3. It is observed that the algorithm shows better performance in the first slices where the heart and the liver can hardly be segmented even with the human eye, the patient datasets with atypical liver shapes and the separation of the tissues in 'low contrast' dataset where the gray level value of the adjacent tissue is very close to the liver. The average AER for the complete dataset is calculated as 9.69%. Figure 4.22 shows the average AER for each patient dataset.

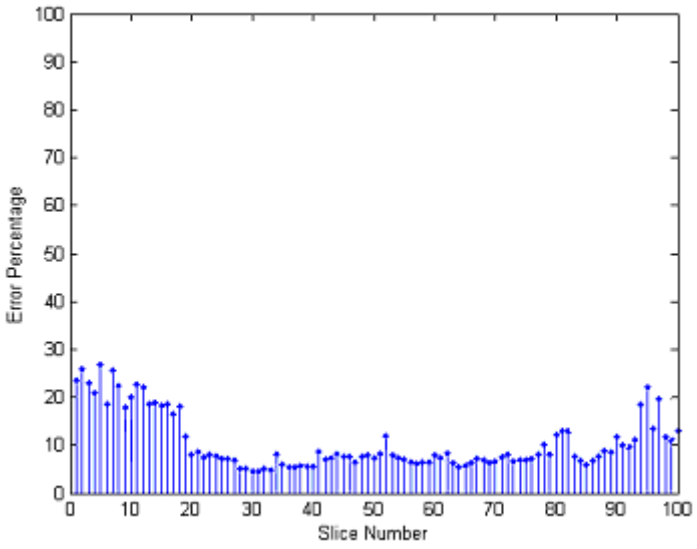


Figure 4.21 Average AER for each slice number

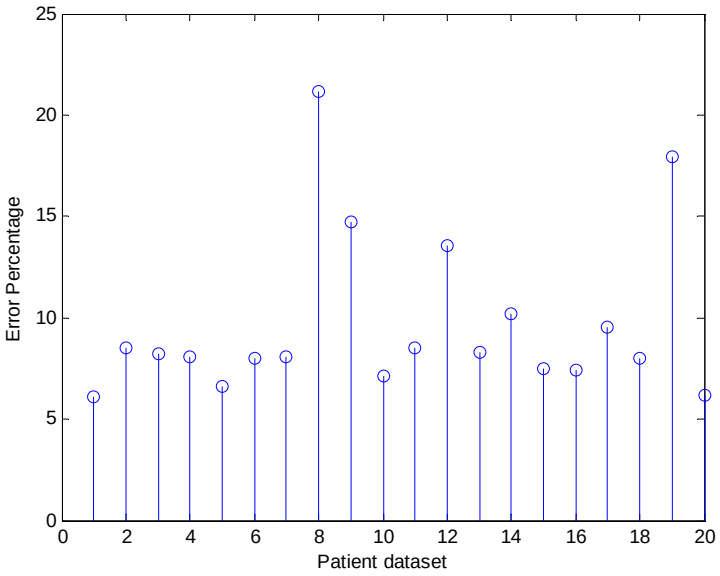


Figure 4.22 AER for CT series

4.4 Comparison of Three Algorithms

Results show that the first algorithm is time efficient for clinical usage, whereas it has high AERs for atypical liver shapes. The second algorithm's ability of parallel adaptation to dataset characteristics increases the tolerance capability of the system and it has better performances for atypical liver shapes such as the datasets of 4, 5 and 11. The third algorithm is both time efficient and has sufficiently good performance. The proposed algorithms give better results especially for atypical liver shapes and low contrast studies where several algorithms fail. The performances of proposed algorithms for 15 datasets are compared in Figure 4.23.

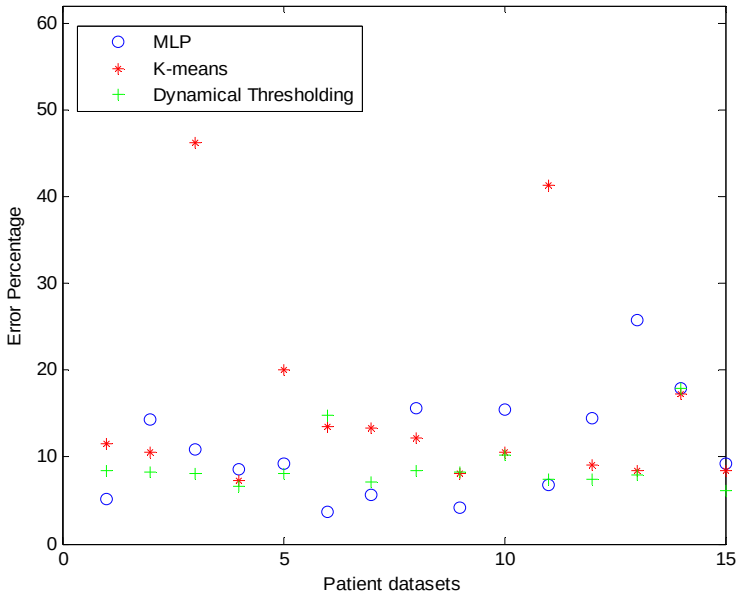


Figure 4.23 Comparison of AERs of three algorithms

CHAPTER FIVE
CONCLUSION

Identifying liver region from abdominal Computed Tomography (CT) datasets is one of the essential steps in visualization prior to the hepatic surgery. However, due to gray level similarity of adjacent organs, injection of contrast media and partial volume effects; robust segmentation of the liver is a very difficult task. Moreover, high variations in liver position, different image characteristics of different CT modalities and atypical liver shapes make the segmentation process even harder. To our knowledge, there is no method in the literature which handles all these difficulties at the same time. In this thesis, three automatic/semi-automatic liver segmentation algorithms that adapt its parameters according to each patient by learning the dataset characteristics to address all the challenging aspects mentioned above are proposed. In the first algorithm, k-means clustering is used to classify liver region. This algorithm learns dataset characteristics prior to the classification process. It takes about 10 minutes with a standard PC (2GB Ram and 3GHz processor). In the second algorithm MLP network is used as a classifier. The robustness of this method follows from its capability of dealing with the contrast variations and atypical liver shapes and this capability is provided by the patient oriented structure of the algorithm. The algorithm learns the dataset characteristics in parallel to segmentation process, and adapts its parameters to these characteristics. This strategy involves a segmentation method which does not utilize a common parameter set found from all patient datasets. Instead, the method is capable of adapting the parameter set to each patient. So the wide ranges of the parameter values are covered and the developed system is robust to several variations in a dataset by adopting its parameters due to the dataset characteristics. The algorithm takes about one and a half hours with a standard PC (2GB Ram and 3GHz processor). In the third algorithm, a dynamical thresholding method which has a slice by slice manner and minimizes the weighted sum of false negative/positive errors is used. . The algorithm takes about half an hour with a standard PC (2GB Ram and 3GHz processor).

Results show that the first algorithm is time efficient for clinical usage, whereas the second algorithm's ability of parallel adaptation to dataset characteristics increases the tolerance capability of the system. The third algorithm is both time efficient and has sufficiently good performance. The proposed algorithms give better results especially for atypical liver shapes and low contrast studies where several algorithms fail.

Areas that may further be examined include speeding up the preprocessing steps, automatic detection of 'initial kidney image', testing different features for representing the liver in a better way and speeding up the convergence of the neural network to increase the performance.

REFERENCES

Acharya, T. & Ray A. K. (2005). Image processing: principles and applications. New Jersey: Wiley-Interscience

Bae, K. T., Giger, M. L., Chen, C. T. & Kahn, Jr. C. E. (1993). Automatic segmentation of liver structure in CT images. *Medical Physics*, 20, 71-78.

Barrett, W. A. & Mortensen, E. N. (1997). Interactive live-wire boundary extraction. *Medical Image Analysis*, 1, 331–341.

Bidaut, L. (2000). Data and Image Processing for Abdominal Imaging. *Abdominal Imaging, Springer Verlag,* 25, 341-360.

Blum, H. A. (1967). Transformation for Extracting New Descriptors of Shapes. Models for the Perception of Speech and Visual Form. W. Wathen-Dunn, (Ed.), (362-380), Massachusetts: MIT Press.

Broelsch, C. E., Emond, J. C., Whitington, P. F., Thistlethwaite, J. R., Baker, A. L. & Lichtor, J. L. (1990). Application of reduced-size liver transplants as split grafts, auxiliary orthotopic grafts, and living related segmental transplants. *Annals of Surgery*, 212, 368-377.

Chou, J. S., Chen, S. Y., Sudakoff, G. S., Hoffmann, K. R., Chen, C. T. & Dachman A. H. (1995). Image Fusion for Visualization of Hepatic Vasculature and Tumors. *Medical Imaging, Image Processing, SPIE Proceedings,* 2434, 157-163.

Fan, S. T., Lo, C. M., Liu, C. L., Yong, B. H., Chan, J. K., Ng, I. O. (2000). Safety of donors in live donor liver transplantation using right lobe grafts. *Archives of Surgery* 135, 336–340.

Gao, L., Heath, D. G., Kuszyk, B. S. & Fishman, E. K.(1996). Automatic liver segmentation technique for three-dimensional visualization of CT data. *Radiology*, 201, 359-364.

Husain, S. A. & Shigeru, E. (2000). Use of neural networks for feature based recognition of liver region on CT images. *Neural Networks for Signal Processing, Proceedings of the IEEE Workshop*, 2, 831-840.

Kawasaki, S., Makuuchi, M., Matsunami, H., Hashikura, Y., Ikegami, T., Nakazawa, Y., et al. (1998). Living related liver transplantation in adults. *Annals of Surgery,* 227, 269–274.

Kiuchi, T., Kasahara, M., Uryuhara, K., Inomata, Y., Uemoto, S., Asonumak, K., et al. (1999). Impact of graft size mismatching on graft prognosis in liver transplantation from living donors. *Transplantation,* 67, 321–327.

Koss, J. E., Newman, F. D., Johnson, T. K., & Kirch, D. L. (1999). Abdominal Organ Segmentation Using Texture Transforms and a Hopfield Neural Network. *IEEE Transactions on Medical Imagin* 18(7), 640-648.

Lee, C. C., Chung, P. C. & Tsai H. M. (2003). Identifying Multiple Abdominal Organs From CT Image Series Using a Multimodule Contextual Neural Network and Spatial Fuzzy Rules. *IEEE Transactions on Information Technology in Biomedicine,* 7, 208-217.

Lim, S. J., Jeong, Y.Y., Ho, Y.S.(2005) Automatic Liver Segmentation for Volume Measurement in CT Images. *Journal of Visual Communication and Image Representation*, 17, 860-875.

Lo, C. M., Fan, S. T., Chan, J. K., Wei, W., Lo, R. J. & Lai, C. L. (1996). Minimum graft volume for successful adult-to-adult living donor liver transplantation for fulminant hepatic failure. *Transplantation*, 62, 696-698.

MacQueen J. (1967). Some Methods for classification and analysis of multivariate observations. *in Proc. 5th Berkeley Symosium on Math. Stat. Prob.,* 281, 1967.

Malago, M., Burdelski, M. & Broelsch, C. E. (1999). Present and future challenges in living related liver transplantation. *Transplantation proceedings*, 31, 1777-1781.

Marcos, A., Ham, J. M., Fisher, R. A., Olzinski, A. T., Posner, M. P. (2000). Single-center analysis of the first 40 adult-to-adult living donor liver transplants using the right lobe. *Liver Transplantation*, 6, 296-301.

Masumoto, J., Masatoshi, H., Yoshinobu, S., Takamichi, M., Takeshi, J., Hironobu N., et al. (2003). Automated Liver Segmentation Using Multislice CT Images. *Systems and Computers in Japan* 34, 2150-2161.

Montagnat J. & Delingette, H. (1996). Volumetric Medical Image Segmentation Using Shape Constrained Deformable Models. *Lecture Notes in Computer Science,* 1205, 13-22.

Ney, D. R., Fishman E. K. & Magid D. (1990). Volumetric rendering of computed tomography data: principles and techniques. *IEEE Computer Graphics & Applications,* 10, 24-32.

Otsu, N. (1979). A Threshold Selection Method from Gray-Level Histograms. *IEEE Transactions on Systems, Man and Cybernetics,* SMC-9, 62-66.

Raia, S., Nery, J. R. & Mies, S. (1989). Liver transplantation from live donors. *Lancet.*, 2, 497.

Seo, K. S., Ludeman, L. C., Park, S. J., & Park. J. A. (2004). Efficient Liver Segmentation Based on the Spine. *ADVIS 2004 Springer Verlag Publisher LNCS*, 3261, 400-409.

Soler, L., Delingette, H., Malandain, G., Montagnat, J., Ayache, N., Clement, J. M., et al. (2005). Fully Automatic Anatomical, Pathological, and Functional Segmentation From CT Scans for Hepatic Surgery., *Academic Radiology,* 12, 1178-1189, 2005.

Tsai, D. (1994). Automatic segmentation of liver structure in CT images using a neural network. *IEICE transactions on fundamentals of electronics, communications and computer sciences*, E77-A, 1892-1895.

Urata, K., Kawasaki, S., Matsunami, H., Hashikura, Y., Ikegami, T., Ishizone, S., et al. (1995) Calculation of child and adult standard liver volume for liver transplantation. *Hepatology,* 21, 1317–1321.

Vincent, L. (1993). Morphological Grayscale Reconstruction in Image Analysis: Applications and Efficient Algorithms. *IEEE Transactions on Image Processing,* 2(2), 176-201.